UNIVERSITY OF WASHINGTON DEPARTMENT OF ORTHOPAEDICS

1995 RESEARCH REPORT

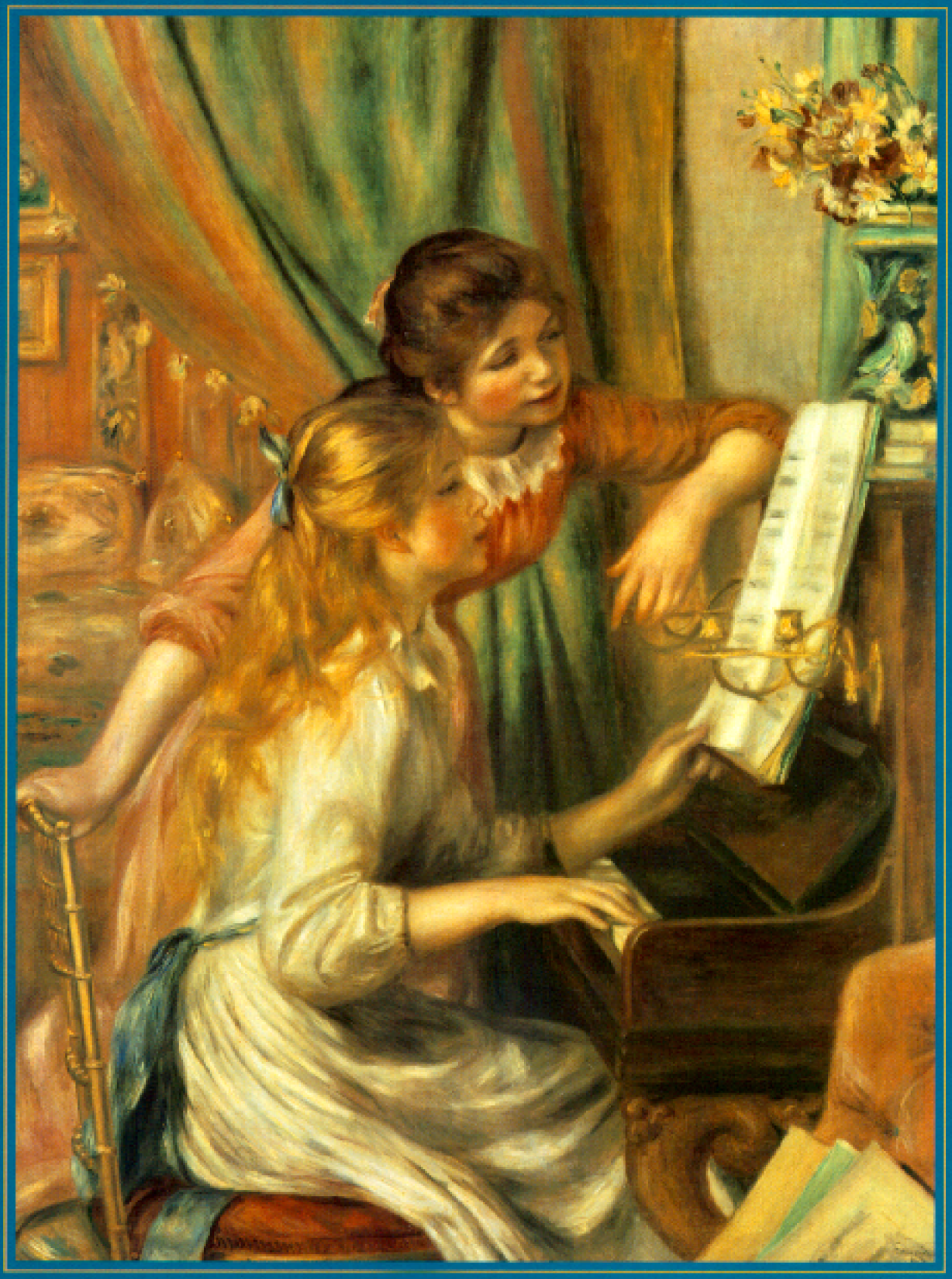

1995 Research Report

Department of Orthopaedics

University of Washington

UNIVERSITY OF WASHINGTON SCHOOL OF MEDICINE

Department of Orthopaedics
University of Washington
Box 356500
Seattle, Washington 98195-6500

Editor: Frederick A. Matsen III, M.D.

Managing Editor: Sandra L. Marvinney

Editorial Assistants: Dee Modest, Susan DeBartolo

Design: Allen L. Auvil

COVER ILLUSTRATION:
"Jeunes filles au piano" by Aguste Renoir is reprinted with permissio of Agence Photographique de la Réunion des Musées Nationaux, Paris, France.

Contents

Chief Resident Abstracts

Foreword

The cover of this year's Research Report shows "Jeunes fines au piano,'' painted by the 51-year-old Pierre Auguste Renoir (1841-1919). In that Renoir suffered from severe rheurnatoid arthritis, this painting is fitting for this issue, which features our many departmental activities related to arthritis. Despite having this "disabling" condition for the last 23 years of this life, Renoir continued to paint, producing many of his greatest masterpieces during that period. This painting also reflects the awe in which we hold so many of our patients, who notwithstanding their major challenges, continue to lead happy and productive lives. As scientists, teachers, and clinicians, it is our privilege to work with them.

This year we celebrate the close relationship we share with the Washington State Chapter of the Arthritis Foundation. We have collaborated with the Arthritis Foundation, Prosthetics Research Study, and the Lockwood Foundation to investigate new methods to educate patients, families, and the public using an interactive multimedia kiosk, which puts a world of information about arthritis at the patient's fingertip. Kiosks are in operation at the Bone and Joint Center at Roosevelt II and at the Arthritis Foundation office. Together with Greg Gardner of the Division of Rheumatology and Basia Belza of the Department of Physiological Nursing, our faculty have collaborated in research and conducted five most well-received public education forums.

This Research Report includes articles on the changes in collagen and ultrastructure in osteoarthritis, the assessment of fatigue in rheumatoid arthritis, the management of osteoporosis, and treatment effectiveness for avascular necrosis of the hip. We also present reports on the management of intra-articular fractures of the acetabulum, scaphoid, spine, and radius. Finally, we include an important long-term follow-up of reconstructions for anterior cruciate ligament deficiency and an article on the superior stability of shoulders.

The strength of the departmental research program is demonstrated by this list of our national grants found on page 41. Our faculty continue to gain recogrution for their research excellence. Linda Sandell has been appointed as Research Career Scientist by the Department of Veteran's Affairs. In association with Linda, Howard Chansky received the Young Investigator's Award from the Orthopaedic Research Society for their work on "A Human Chondrosarcoma Cell Line with a Mutation of the p53 TumorSuppressor Gene." Michele Battie won the 1995 Volvo Award in Clinical Sciences for her work on "Determinants of Disc Degeneration." We also congratulate Michele as she becomes professor and chair of the Department of Physical Therapy at the University of Alberta, Edmonton.

Doug Harryman received the American Shoulder and Elbow Surgeon's 1995 Traveling Fellowship. Peter Simonian received the American Orthopaedic Association-Zimmer 8th Annual Travel Award.

Welcome to Sohail Mirza, who will be joining our Spine Service. A 1994 graduate of the residency program, he received the Daniel E. Hogan Fellowship in Spine Surgery at Harvard Medical School, and has been working with Augustus A. White for the past year.

We also welcome back 1991 graduate Kit Song and his wife Carol. Kit will be working with Vince Mosca at Children's Hospital.

This year, our Resident Research Days guest professor is Dr. Wayne Akeson from San Diego, California. Dr. Akeson is a former member of our faculty and father of one of our graduates, Jeff, who now lives in Peoria, Illinois. ResidentResearch Days are supported by the University of Washington Orthopaedic Alumni and by a Fred W. Hark, M.D., and William A. Hark, M.D. Lectureship Award from OREF. Our thanks to the many alumni who contribute to support this and other key activities for the residents.

Finally, let me express our deepest gratitude to those friends and patients who have made donations to our research program. Their generosity has provided critical support for our research programs in arthritis and related musculoskeletal conditions.

Frederick A. Matsen, III, M.D.
Professor and Chair

Monitoring Bone Resorption in Early Postmenopausal Women Using an Immunoassay for Collagen Degradation Products

David R. Eyre, Ph.D.

Osteoporosis is a major public health problem. The combined societal costs from femoral neck fractures alone exceed $10 billion annually in the United States. New treatments, preventive therapies, and improved diagnostic methods are being pursued worldwide. We summarize recent findings on the clinical value of a new biochemical marker for monitoring the level of bone resorption in postmenopausal women. Part of the work was published as a collaboration stemming from a clinical trial of an advanced form of bisphosphonate, alendronate (Gertz et al., 1993).

The method for quantifying bone resorption developed from long-term basic research to understand the molecular mechanisms of cross-linking in collagen. It relies on a monoclonal antibody to quantify by immunoassay a specific fragment of type I collagen excreted in urine. This peptide analyte (NTx) is derived from an N-telopeptide cross-linking site that links collagen molecules in the organic matrix of bone. The NTx peptide is particularly resistant to further proteolysis when bone collagen is degraded as part of the normal process of bone resorption by osteoclasts (Figure 1).

Osteoclastic bone resorption is a continual activity in the normal skeleton, a mechanism of both structural remodeling and calcium homeostasis. At menopause, when ovarian production of estrogen falls, osteoclastic resorption can increase dramatically, causing rapid loss of bone mass in some women. Through the cellular mechanisms that couple bone formation and resorption, the formation rate also eventually increases. However, the lag time and net imbalance between resorption and formation can result in a significantly accelerated rate of loss of bone mass. Identifying women who are high resorbers, and hence potentially fast losers of bone, is a promising application for any biochemical test that is specific for osteoclast activity.

A second application, perhaps of most immediate value, is in monitoring the effectiveness of therapeutic agents that inhibit osteoclast activity. Bisphosphonates are a class of compound that can selectively inhibit osteoclasts actively engaged in resorbing bone. Recent findings show that the NTx assay is a highly specific monitor in human subjects of both the increase in bone resorption activity that occurs at menopause and the inhibition of resorption on bisphosphonate treatment.

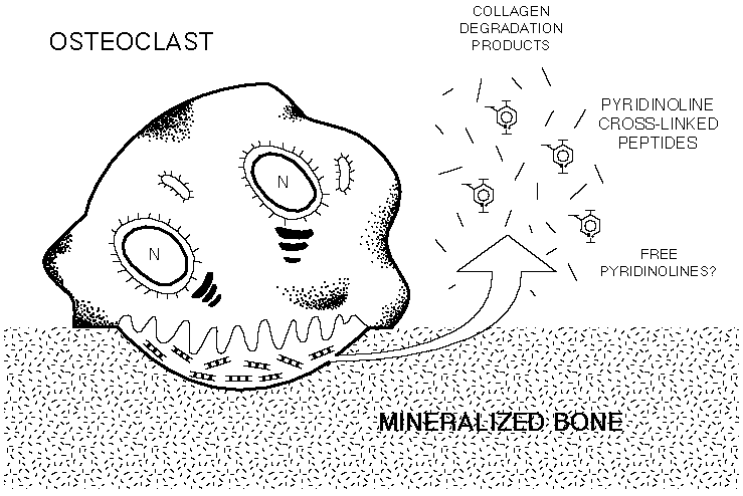

FIGURE 1: Osteoclasts resorb mineralized bone by removing mineral and degrading the collagenous matrix by proteases. The NTx peptide analyte is derived from a pyridinoline cross-linking site in bone type I collagen.

Postmenopausal Increase in Bone Resorption

Figure 2 compares scatter plots of cross-sectional data from age-matched premenopausal and early postmenopausal women. These urinary NTx measurements (normalized to creatinine to correct for urine concentration) show a 2.5-fold higher mean value and a much greater range after menopause. About one-third of subjects resorb bone at a level two standard deviations above the premenopausal mean. This group of women lose bone mass faster than do those still in the premenopausal range.

Suppression of Bone Resorption by Alendronate

In a clinical trial to evaluate the effects of different doses of the bisphosphonate, alendronate sodium early postmenopausal women were monitored for various markers of bone metabolism (Gertz et al., 1993). The results showed that urinary NTx measurements were highly responsive and dose dependent (Figure 3). When therapy stopped after six weeks, the urinary marker of bone resorption returned toward baseline

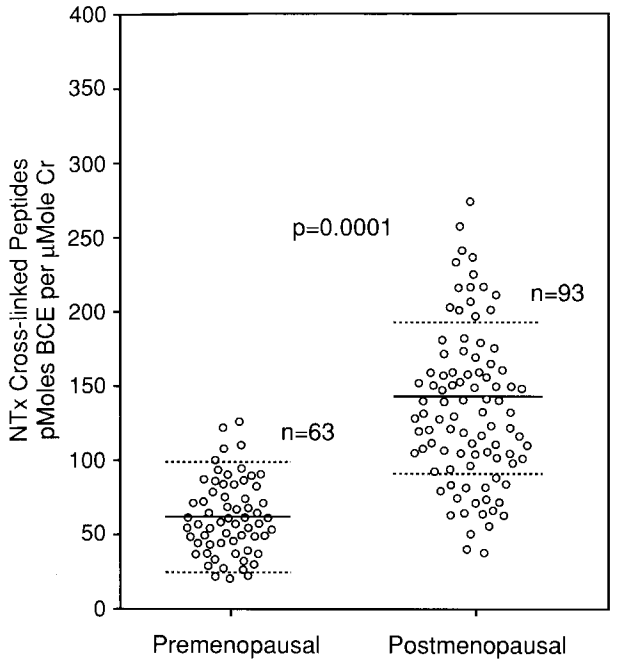

FIGURE 2: Urinary excretion of cross-linked N-telopeptides in age-matched premenopausal vs. early postmenopausal women.

values as evidenced by the measurements at 30 weeks.

This study also showed a correlation between baseline excretion of the NTx peptide and lumbar spine bone mineral density (BMD), both with baseline measurements and changes in BMD over time. In conclusion, the results show that this new ELISA (immunoassay) for quantifying urinary cross-linked peptides of collagen is the most sensitive and specific biochemical marker for bone resorption available. The test has potential value in monitoring the response of individual patients to antiresorptive therapy, for example in assessing whether osteoclast activity has been returned to an acceptable premenopausal range. Studies are also in progress to determine to what degree the test may be useful for screening women at menopause for an increased risk of future osteoporotic fracture.

Supported by a grant from Ostex International, Inc., Seattle, Washington, and the Burgess Chair for Orthopædic Research.

Recommended Reading

Bollen A-M, Eyre DR: Bone resorption rates in children monitored by the urinary assay of collagen type I cross-linked peptides. *Bone*, 15:31-34, 1994.

Gertz BJ, Shao P, Hanson DA, Quan H, Harris ST, Genant HK, Chesnut CH III, Eyre DR: Monitoring bone resorption in early postmenopausal women by an immunoassay for cross-linked collagen peptides in urine. *J Bone Miner Res*, 9:135-142, 1994.

Hanson DA, Weis M-A E, Bollen A-M, Maslan SL, Singer FR, Eyre DR: A specific immunoassay for monitoring human bone resorption: Quantitation of type I collagen cross-linked N-telopeptides in urine. *J Bone Miner Res*, 7:1251-1258, 1992.

Rosen HN, Dresner-Pollak R, Moses AC, et al: Specificity of urinary excretion of cross-linked N-telopeptides of type I collagen as a marker of bone turnover. *Calcif Tissue Int*, 54:26-29, 1994.

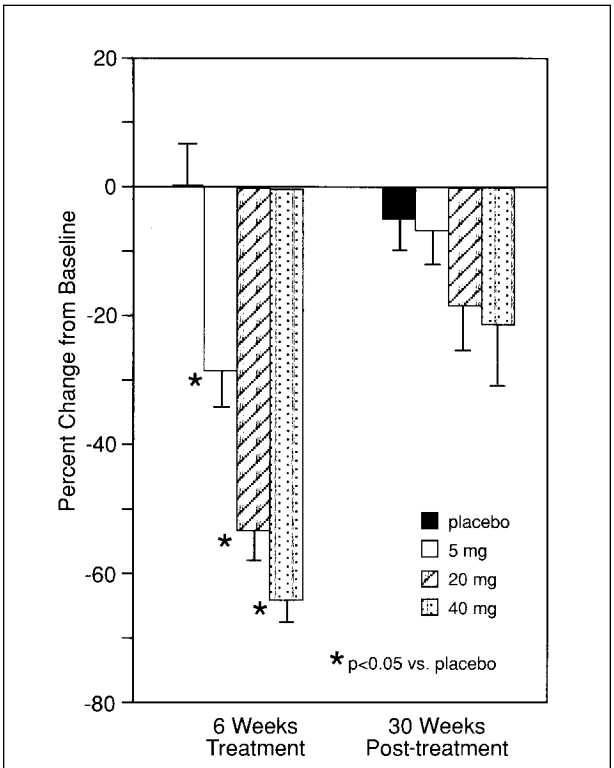

FIGURE 3: Effect of alendronate treatment on the urinary excretion of cross-linked collagen peptides. Mean results are given for the percentage change from baseline after a six-week treatment with 0, 5, 20 or 40 mg alendronate daily, and also 30 weeks after treatment ceased. Values are means + SEM. (n = 16/17/group), *p <0.05 versus placebo.

Discoordinate Gene Expression of Aggrecan and Type II Collagen mRNA in Experimental Osteoarthritis

John Matyas, Ph.D.*
Linda J. Sandell, Ph.D.

Articular cartilage is composed primarily of type II collagen and the large aggregating proteoglycan aggrecan, endowing cartilage with its unique material properties. In end-stage osteoarthritis (OA), articular cartilage is disrupted and aggrecan concentration is reduced in the remaining cartilage. This observation led early workers to conclude that articular cartilage degeneration and malfunction was due to degradation of aggrecan. In contrast to endstage OA, in vivo and in vitro models reveal that proteoglycan synthesis is actually *increased* in cartilage in early OA. Furthermore, a feature of early experimental OA is *increased* cartilage mass, which is due in part to an increase in aggrecan. Collagen synthesis is also increased in human and canine cartilage in osteoarthritis.

Recently, studies have shown that some chondrocytes in osteoarthritic cartilage produce high levels of type II collagen mRNA and proteoglycan, whereas others produce neither. This finding was interpreted as a coordinated synthesis of aggrecan and type II collagen. For proper repair, coordinated synthesis would be advantageous because restoration of the matrix presumably requires newly synthesized aggrecan and type II collagen in the proper proportions; uncoordinated synthesis, however, could be a crucial event in the pathogenesis of osteoarthritis.

Methods

In this study, five skeletally mature, mixed-breed, male dogs (30-35 kg) received dog chow and water ad libitum, were kept in kennels (2.5 x 1 x 2 meters, L x W x H), and were supervised by a veterinarian. The anterior cruciate ligament (ACL) of one stifle (= knee) joint of each animal was transected through a lateral arthrotomy; the contralateral stifle served as an unoperated control. Animals were euthanized 10 weeks after surgery.

Cartilage was shaved from the articular surfaces of each stifle, with care taken to avoid marginal and osteophyte tissues. Shavings were placed into polypropylene tubes filled with liquid nitrogen. Excess nitrogen was poured off and the frozen "wet" mass of the shavings was measured before being powdered in a Spex™ Freezer Mill.

To monitor gene expression of aggrecan and collagen, RNA was isolated from cells. Purified RNA was separated by gel electrophoresis and blotted to nylon membranes. cDNA probes for type II collagen and the G3 and KF domains of aggrecan were used to measure the mRNA levels.

Results

We observed no cartilage lesions at the time of surgery and encountered no surgical complications. At necropsy, no arthritic lesions were found in the hip, ankle, or contralateral stifle joints. In all control joints a trace of synovial fluid was present, the ACL was intact, and the cartilage was shiny and blue. All operated joints had blunt ACL stumps, copious synovial fluid, marginal osteophyte formation, and dull, opaque-white articular cartilage. Cartilage mass was significantly greater in operated joints compared to controls (Figure 1). The ethidium bromide-RNA fluorescence and relative autoradiographic signals for the G3, KS, and COL2 probes are shown in Figure 2.

Discussion

Our study reveals that the gross morphological changes in the joint and the hypertrophy of the osteoarthritic cartilage are similar to findings of previous studies and confirm the stage of the disease process in this model. Although cartilage hypertrophy is characteristic of operated joints in this model, chondrocyte hyperplasia is not because the overall DNA content is unchanged and the concentration of DNA in the tissue actually diminishes. Our findings for cartilage DNA concentration at this relatively early stage of OA, in which cartilage fibrillation is absent and chondrocyte cloning is moderate, are consistent with the overall decline in chondrocyte numerical density measured at this time in this model.

The findings of this study are difficult to compare directly with previous in vivo and in vitro studies of aggrecan and collagen synthesis. First, most studies of synthesis have employed radiosulfate and tritiated proline as precursors, which may be incorporated "nonspecifically" and hence are not entirely precise indicators of aggrecan and type II

(continued on page 6)

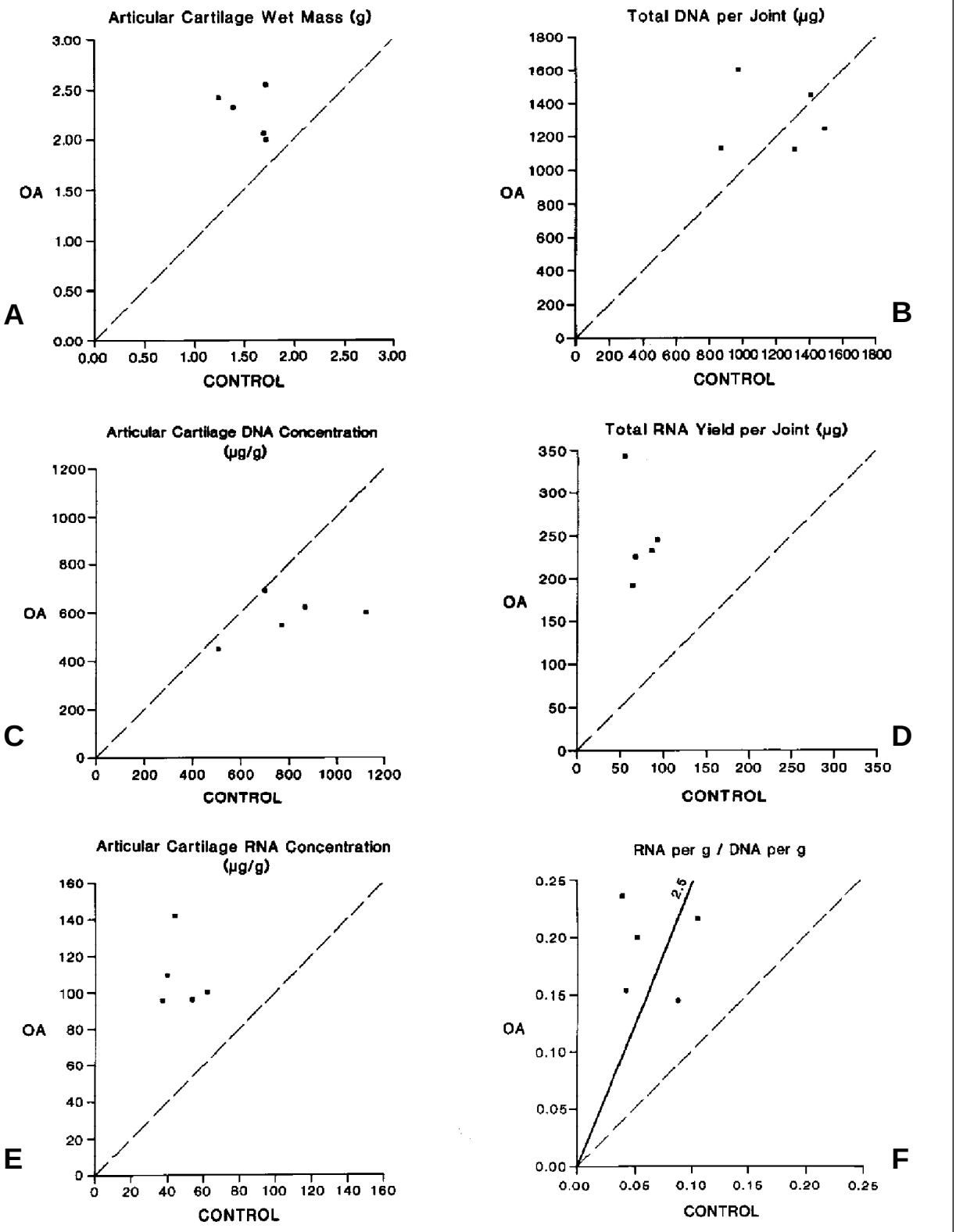

FIGURE 1: (**A**) All the points lie above the line of identity, indicating cartilage hypertrophy in operated joints. The total amount of DNA per joint was not significantly different between osteoarthritic and control joints (**1B**), yet the mass was greater; thus, the concentration of DNA per gram of articular cartilage was significantly lower in osteoarthritic than in control joints (**1C**). In contrast, the total RNA per joint (**1D**), the concentration of RNA per gram of articular cartilage (**1E**), and the concentration of RNA normalized to DNA concentration (**1F**) were all significantly elevated in cartilage from osteoarthritic joints.

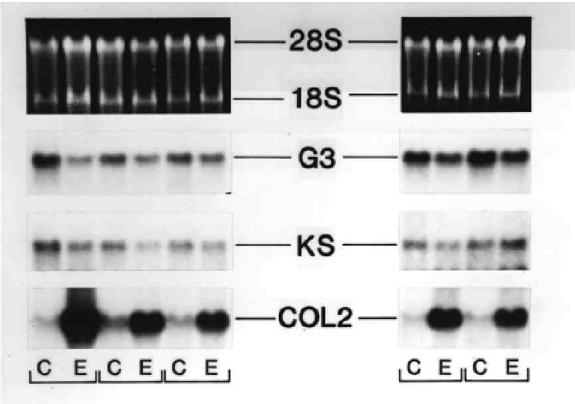

FIGURE 2: The ethidium bromide fluorescence and autoradiographs of hybridizations with a variety of cDNA probes (canine glyceraldehyde-3-phosphate dehydrogenase, human elongation factor-1, and human 18S rRNA) confirmed that a similar amount of total RNA was loaded in all lanes (data not shown). G3 and KS are lower in osteoarthritic cartilage than in controls; COL2 is higher than in controls. When data are normalized to DNA concentration the results change dramatically: the average signal for aggrecan core protein (KS and G3) is increased twofold and type II procollagen is increased eight-fold in operated joints compared to controls. Paired t-tests reveal that all three signals are significantly elevated in osteoarthritic cartilage.

collagen synthesis. Second, variability in aggrecan post-translational glycosylation and sulfation complicate comparisons of mRNA and radiosulfate data. Third, differences in the rates of tissue penetration, diffusion, and incorporation of radiolabelled precursors between control and osteoarthritic cartilages are difficult to quantify and hamper any comparison with mRNA data.

Thus, to the best of our knowledge, the absolute levels and the absolute ratios of aggrecan core protein and type II collagen synthesis are unknown in either normal or osteoarthritic cartilage. Indeed, these studies are capable only of reporting relative changes in the levels and ratio of aggrecan and type II collagen mRNA. Despite these concerns, it is remarkable that the magnitude of changes in aggrecan and type II collagen mRNA observed in our study are similar to previous reports in which aggrecan synthesis is elevated approximately twofold and type II collagen synthesis is elevated approximately 10-fold in early canine experimental OA. These similarities suggest that synthesis of aggrecan and type II collagen is predominantly regulated at the level of gene transcription.

The increase in aggrecan mRNA is consistent with increases in aggrecan proteoglycan concentration in the extracellular matrix of osteoarthritic canine cartilage. That the signals of the G3 and KS probes were comparable suggests that the aggrecan core protein is completely translated in osteoarthritic cartilage and that aggrecan fragments lacking G3 are most likely products of extracellular degradation.

Although aggrecan breakdown products and "proteoglycanase" activity appear to be elevated in OA, it seems that, at least at this early time, the overall balance between the anabolism and catabolism of aggrecan proteoglycan favors anabolism because there is a net accumulation of aggrecan in the matrix. Unlike aggrecan, the anabolism and catabolism of collagen appear to be in balance because type II collagen does not accumulate in osteoarthritic cartilage despite a large increase in the level of type II collagen mRNA and in hydroxyproline incorporation.

These observations suggest that collagen catabolism or exportation from the tissue is accelerated in OA. This conclusion is consistent with reports of increased collagenolytic activity, increased collagenolytic enzyme levels, and a relative decrease in enzyme inhibitors in osteoarthritic cartilage. These observations are also consistent with reports that type II-collagen-specific breakdown products are elevated in osteoarthritic cartilage.

The relative proportion of aggrecan and type II collagen in articular cartilage determines its functional quality and changes in this proportion undoubtedly influence its functional behavior. Our study documents that while both mRNAs are increased, the levels of aggrecan core protein and type II procollagen mRNA are disproportionate in the early phase of OA in this animal model. The results suggest that disproportionate synthesis of aggrecan core protein and type II collagen is a metabolic characteristic of early OA that may contribute to its pathogenesis in this model.

Our study supports the view that OA is a metabolic disturbance of articular cartilage. Because the half-life of collagen protein is relatively long compared to aggrecan proteoglycan, it is unclear from these studies of a single time point if the observed discoordinate gene expression ultimately results in OA. We speculate that a persistent imbalance between the anabolism and catabolism of collagen and aggrecan may contribute to the pathogenesis of osteoarthritis and that the gene expression of these molecules may exacerbate this imbalance.

Recommended Reading

Adams ME, Brandt KD: Hypertrophic repair of canine articular cartilage in osteoarthritis after anterior cruciate ligament transection. *J Rheumatol*, 18:428-435, 1991.

Eyre DR, McDevitt CA, Billingham MEJ, Muir H: Biosynthesis of collagen and other matrix proteins by articular cartilage in experimental osteoarthrosis. *Biochem J*, 188:823-837, 1980.

Lohmander LS, Neame PJ, Sandy JD: The structure of aggrecan fragments in human synovial fluid: Evidence that aggrecanase mediates cartilage destruction in inflammatory joint disease, joint injury, and osteoarthritis. *Arth Rheum*, 36:1214-1222, 1993.

Mankin, HJ, Dorfman, H, Lippiello, L, Zarins, A: Biochemical and metabolic abnormalities in articular cartilage from osteoarthritic human hips. *J Bone Joint Surg*, 53A:523-537, 1971.

**John Matyas, Ph.D., McCaig Center for Joint Injury and Arthritis Research, University of Calgary, Alberta, Canada*

Scanning Electron Microscopy of Arthritic Human Articular Cartilage

John M. Clark, M.D., Ph.D.

Fibrillation and "malacia" are the terms commonly used to describe the gross characteristics of degenerative articular cartilage. By formal dictionary definition and common usage, malacic cartilage is soft and dull in appearance. Fibrillation specifically refers to the presence of fibril-like fronds within or on the articular surface or an affinity for India ink. Surgeons often use these specific terms to describe an arthritic joint surface. They are also used to classify the extent of disease in many scientific articles dealing with the properties of human articular cartilage.

What causes cartilage to appear fibrillated or malacic? Looking through papers on the subject of arthritic cartilage, we could find no answer to this question. Most of the visible damage to cartilage reflects disruption of its fibrous collagen framework, and until recently, the normal collagen arrangement has been poorly understood. The University of Washington Orthopaedic Morphology Unit has used scanning electron microscopy (SEM) to show how normal cartilage structure is based on collagen fibers that rise from the bone and continue into the surface. In that model, collagen fibers rise vertically from the calcified zone, through the radial zone, and then arch over to form the superficial, tangential zone (Figure 1). In this study, we examined normal and arthritic human cartilage to see whether grossly visible abnormalities are associated with specific patterns of disruption within the collagen fiber network.

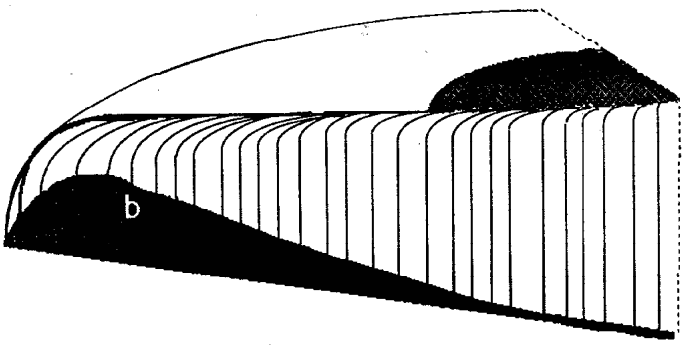

FIGURE 1: Diagrammatic representation of the collagen fiber anatomy in a tibial plateau. In the periphery, the radial collagen fibers run from the bone (b) to the surface where they turn and form the lamellae of the tangential layer. In the center (shaded) the radial fibers may arch somewhat but do not form lamellae. There, the surface is thin and softer than that of the periphery.

Methods

The material for this study was cartilage from the patella, femoral condyle, and tibial plateau of 22 persons, aged 13 to 85. The specimens were removed at autopsy (18 knees) or during routine primary joint replacement (10 knees). In most knees sampled for this study, some or all of the articular surfaces were not smooth. Samples of cartilage were removed from areas that were grossly smooth and hard (normal), softened but smooth (malacic), and overtly fibrous (fibrillated). Those taken from the patients with knee replacements were classified as "osteoarthritic." Those taken at autopsy were classified as "normal young" or "normal old." Smooth-appearing specimens were brushed with India ink, and those stained with ink were marked as such.

We removed centimeter-square specimens from all joints, prepared them for SEM, and recorded the gross appearance of each sample. The samples were broken open using a freeze-fracture method to provide a view of the inner structure of the cartilage. Thus, we could examine both the articular surface as well as the deep collagen framework and compare the features observed by SEM to their gross appearance.

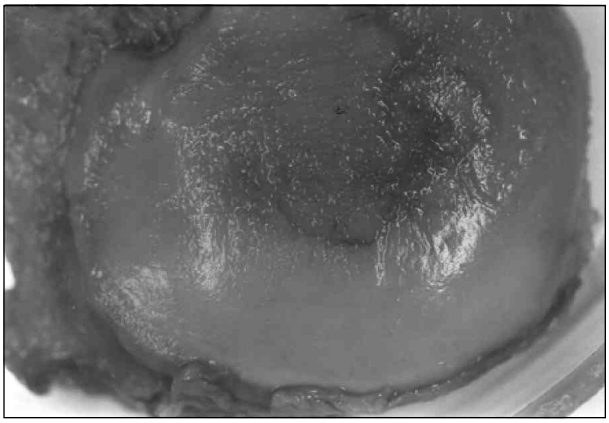

FIGURE 2A-B: The gross appearance of malacia. **A** (right): Medial tibial plateau of a normal 42-year-old man. The periphery is normal, i.e., hard and smooth. The center is "malacic" in that it is soft and dull. It also stained with India ink. **B** (below): Diagram of the changes that accompany malacia. Fissures have formed between the collagen fibers near the surface. At the center, these fissures extend into the surface and create a roughened appearance. In the periphery, the cartilage has become slightly soft.

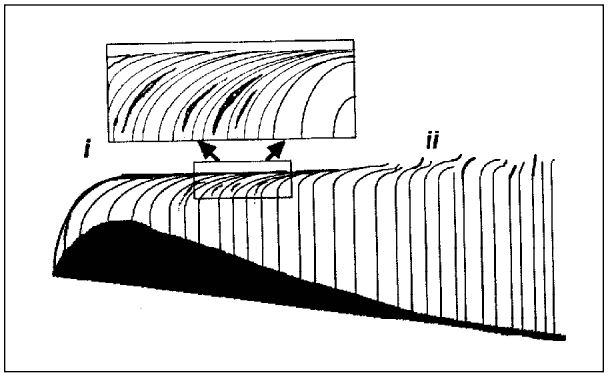

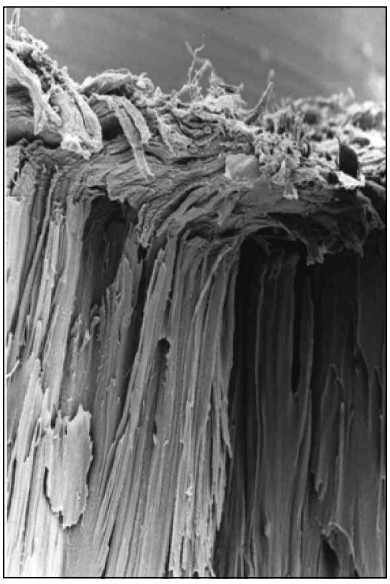

FIGURE 2C-D**: C** (below)**:** Micrograph showing fissures between fibers in the subsurface region in the periphery of a tibial plateau with gross characteristics of malacia (softness and a somewhat dull patina). **D** (right): Micrograph shows the exposed ends of collagen fibers in the center of a malacic plateau.

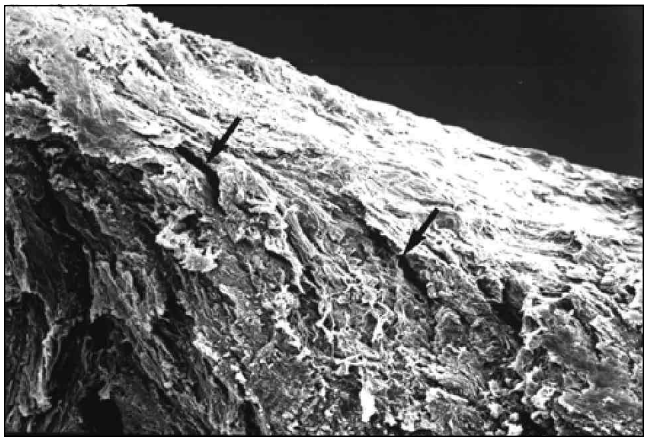

Results

In young, normal subjects, the femoral condyles and periphery of tibial plateaus were hard and shiny. The central tibial plateaus and the patellas were soft and dull, but did not show gross fissuring or fronding. All specimens from arthritic and older normal subjects had some superficial roughness (Figure 2A). The femoral condyles of normal older subjects were firm but dull. The centers of their tibial plateaus and patellas were softer than those of the young normals, and could be stained with ink. The gross appearance of some arthritic specimens was similar to that of the older normals, but most of the articular surfaces showed fissures, fronding, and / or overt thinning and erosions down to bone.

Normal Tissue: Microscopically, the three-dimensional matrix structure of young normal subjects was identical to that described in our previous studies.

Abnormal Cartilage: Several distinct patterns of abnormality were observed in the collagen matrix of the osteoarthritic and older specimens. Generally, these patterns correlated well with their gross appearance.

Malacia (Softening and Dullness)

Joint surfaces initially classified as *malacic* because of softening and a dull appearance were found by microscopy to have either superficial or subsurface fissures between the collagen fibers (Figure 2B-C). Surfaces that were grossly dull and stained with ink appeared rough when seen at magnifications greater than 50X. This roughness was created by the exposed ends of collagen fibrils (Figure 2C). The vertical fractures showed that these fibrils were the free ends of deep radial collagen fibrils (Figure 2B). This pattern was seen only in the central plateau and patellae where the tangential layer is normally quite thin.

Subsurface Fissures: In other soft, dull specimens, the articular surface was microscopically smooth, but the tangential lamellae and / or vertical fibers beneath the surface were separated by clefts. These clefts followed the planes between the collagen fiber systems (Figure 2D). They were most commonly observed in the deep aspect of the tangential zone, and occasionally extended from the tangential layer down into the most superficial fifth of the

cartilage thickness. The fissures often contained flocculent material with the morphologic features of precipitated joint fluid. These specimens did not stain with ink.

Fibrillation

The gross appearance of *fibrillation* was created by complete delamination of the tangential zone or deep fissuring between the radial collagen fibers.

Superficial Fronding: On gross inspection, fronds of cartilage appeared to project from the surfaces of many of the osteoarthritic specimens (Figure 3A). SEM of vertical fractures through these areas demonstrated that such fronds were formed by tangential lamellae that had separated from the articular surface (Figure 3B). Usually, these free sheets of collagen had folded upon themselves, taking a cylindrical form. This phenomenon occurred in locations normally covered by tangential layer, e.g., the peripheral tibial plateau and femoral condyles.

Full-thickness Fissures: In the most badly damaged osteoarthritic specimens, fissures passed through the articular surface and penetrated deeply into the radial zone. Where a well-established tangential layer had been present, these fissures were accompanied by superficial fronding (Figure 4A-B). Deep fissures sometimes extended to the subchondral bone, but only where the cartilage was severely damaged.

Discussion

Several articles have reported on the SEM appearance of osteoarthritic and rheumatoid human articular cartilage. All describe some disruption of the collagen matrix, but none contrast pathologic changes to a widely accepted concept of normal collagen matrix anatomy. Therefore, this is the first study to define the microscopic features of malacia and fibrillation.

Our findings show that patterns of damage to articular cartilage can be interpreted in terms of our modified version of the classic Benninghoff model of matrix fibrous anatomy (Figure 1). Dullness and softness (i.e., malacia) of grossly intact articular surfaces reflect the presence of narrow clefts among the superficial ends of vertical or tangential collagen fibers. Where the tangential layer is very thin or nonexistent, as in the central tibial plateau, the patella, and the perifoveal region of the femoral head, the surface is often disrupted, thus leaving the free ends of radial collagen fibers exposed. Gross fronding (i.e., fibrillation) is caused by separation and displacement of the large collagen fibers that form the lamellae of the tangential zone and the deep vertical fibers of the radial zone. Fronding that extends above the plane of intact areas (an appearance familiar in arthroscopy) is caused by delamination of the tangential layer. Full-thickness fibrillation is apparent when the deep radial fibers are also exposed. India ink will stain any surface through which subsurface fissures have opened.

These observations imply that the collagen fiber framework of articular cartilage is progressively destroyed as degenerative arthritis worsens. The first change visible by microscopy is splitting apart among the superficial ends of the large vertical collagen fibers. As the degeneration proceeds, the extent of the fissures increases, both upward

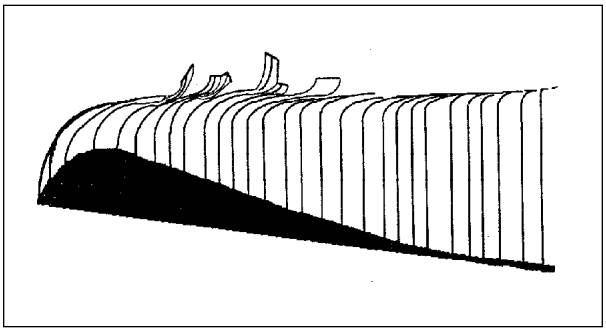

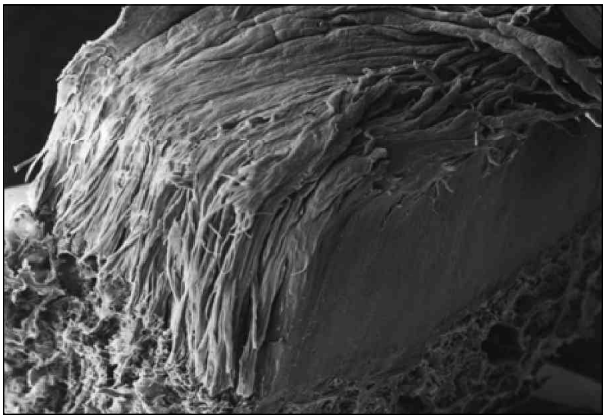

FIGURE 3A-B: Superficial fibrillation. **A** (upper): The diagram shows how delamination of the superficial collagen lamellae can create fronds that project out from the surface of the articular cartilage. **B** (lower): Micrograph of femoral condyle that had superficial fronding. The fractured surface at left shows that these fronds are extensions of the deep radial collagen fibers that originally had formed the joint surface. Cut surface at right shows that the deep part of the cartilage is still solid and intact, indicating that this type of fronding occurs in relatively sound cartilage (bar = 1000 m).

FIGURE 4A-B: Fibrillation caused by deep fissures in degenerative cartilage. **A** (right)**:** This diagram shows that fibrillation can also occur when the deep radial fibers become separated. In the periphery (left), the surface has fronds or blisters. **B** (above)**:** View looking down on a tibial plateau with deep fissures, the surface is very rough and the fronds are more displaced. Deep fissures are also seen here.

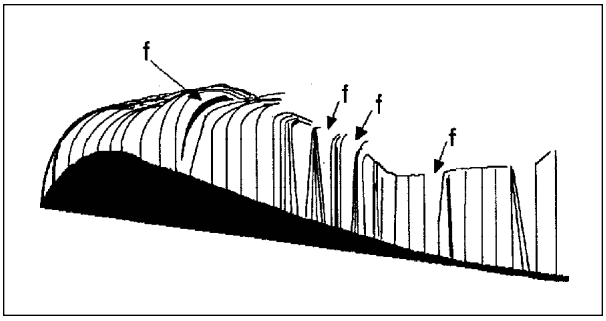

TABLE 1: Structural Changes Observed at Various Stages of Arthritis and in Different Locations

	Center of Tibial Plateau	Peripheral Plateau / Femoral Condyles
Gross Appearance		
Normal young	soft and dull	firm and shiny
Normal old	soft and dull	firm but dull
Mildy arthritic	soft and dull	softening, but superficial fronds
SEM Findings		
Normal young	smooth, no tangential layer	smooth with an intact tangential layer
Normal old	fissures among fibers at surface	roughness of surface
Mildly arthritic	more extensive fissures at surface	fissures among tangential lamellae in surface

(if a tangential surface layer exists) and downward toward the bone (Figure 2). Deep splitting occurs later in the disease process and is evidently a far more serious injury, because it usually is accompanied by erosion, that is actual loss of the cartilage substance. Discovering why the collagen fibers separate (too much load, breakdown of chemical bonds, loss of hydrostatic pressure) will be a significant step.

For a clinician, the most important finding here is that softness, dullness, and even superficial fronding can exist in the absence of severe damage to deep collagen matrix. India ink staining is nonspecific. The conditions that afflict the patellar articular surface are probably too diverse to justify broad use of the term "chondromalacia."

Recommended Reading

Clark JM: The organization of collagen fibrils in the superficial zones of articular cartilage. *J Anat*, 171:117-130, 1990.

Dorland's Illustrated Medical Dictionary, 27th ed. WAN Dorland (ed). Philadelphia: W.B. Saunders Co., 1988.

Meachim G: Light microscopy of Indian ink preparations of fibrillated cartilage. *Ann Rheum Dis*, 31:457-464, 1972.

Outerbridge RE: The etiology of chondromalacia patellae. *J Bone Joint Surg*, 43B:752-757, 1961.

Stedman's Medical Dictionary, 25th ed. WR Hensyl (ed). Baltimore: Williams and Wilkins, 1990.

Traber's Cyclopedic Medical Dictionary, 17th ed. CL Thomas (ed). Philadelphia: F.A. Davis, 1993.

Walker PS, et al: Behavior of synovial fluid on surfaces of articular cartilage: A scanning electron microscope study. *Ann Rheum Dis*, 28:1-14, 1969.

Fatigue: An Underappreciated Symptom in Rheumatic Disease

Basia Belza, Ph.D., R.N.

Why is it that the symptoms we see the most, we understand the least? Fatigue is a frequently occurring problem and its impact on society is staggering. Indirect costs for fatigue-related lawsuits and loss of productivity are significant. Results from the National Health and Nutrition Examination Survey indicate that 14% of the men and 20% of the women responding to the survey reported experiencing fatigue in a one-week period. Fatigue accounts for more than 10 million office visits and $300 million in medical care costs per year. Yet, our understanding of the mechanisms of and effective treatment for fatigue remains limited. As clinicians and researchers, we need to increase our attention to fatigue as it has the potential to interfere with rehabilitation efforts, work productivity, and personal safety.

For the healthy person, fatigue usually results from an identifiable event: a busy day at work, strenuous physical exercise, or emotional tension. Fatigue that healthy adults experience is usually resolved by rest. Both the fatigue and the ensuing recovery period are normal experiences. Fatigue is rarely considered a serious problem because the duration is temporary and the relief measures are effective.

In contrast, for persons with a chronic condition, a single cause of fatigue and an effective remedy to lessen it may not be so apparent. A good night of sleep alone may not completely relieve the fatigue and the fatigue condition may not be transient. For those who are chronically ill, fatigue does not resolve easily. As such, the experience of fatigue is different for the person who is healthy versus the person who has a chronic illness.

Studies Assessing Fatigue

We have been particularly interested in studying the impact of fatigue in rheumatoid arthritis (RA). Although many of the effects of the disease are located in the joints, the systemic nature of RA produces extra-articular symptoms such as fatigue, which exists in all gradations of the disease and typically increases during flares and decreases during remission. Our studies show that fatigue occurs in 93% of subjects with RA. Although the absence of fatigue is one of the criterion for clinical remission, the presence of fatigue is not a criterion for diagnosis.

In our initial studies, we measured fatigue scores with the Multidimensional Assessment of Fatigue (MAF) scale in which 0 represents no fatigue and 50 represents severe fatigue. The purpose of this particular study was to compare fatigue in persons with RA with age- and gender-matched controls without RA. Subjects with RA reported significantly higher levels of fatigue (mean=28) compared to healthy controls (mean=16). Fatigue did not change significantly in either the RA or control group over time. Fatigue was strongly associated with poor sleep, functional disability, greater pain, more depressive symptoms, and lower hematocrits.

In another study, we measured the dimensions and correlates of fatigue in a sample of 133 older adults with RA. They reported that significant fatigue occurred every day, stayed at the same during the course of the week, and most often affected walking and doing household chores. A hierarchical multiple regression model explained 61% of the variance in fatigue. Variables making substantial contributions to the variance in fatigue were pain (19%), gender (13%), sleep quality (8%), physical activity level (6%), comorbid conditions (4%), and functional status (4%). We found that the profile of the person at high risk for fatigue is likely to be a woman recently diagnosed with RA who has several comorbid conditions, a high level of pain, sleeps poorly, engages in little or no physical activity, and has functional limitations.

We are now conducting a preliminary test of the effects of a Fatigue Modulation Program (FMP) as an intervention for persons with RA. We are testing the feasibility of implementing a three-dimensional FMP (symptom monitoring, activity pacing, and routine exercise) for those with moderate to high levels of fatigue and are determining the effects of the intervention on perceived fatigue, exercise tolerance, and functional status. We will use a two-group randomized experimental design with an intervention group (n=24) receiving instruction on symptom monitoring, activity pacing, and participating in a 12-week aerobic exercise class while the control group (n=24) participates in a 12-week non-aerobic (range of motion) class.

To date, nine subjects have been enrolled in the study and completed human performance tests (exercise tolerance tests). Results from this study will increase our efforts to understand the mechanisms of fatigue and to develop effective intervention strategies for amelioration or elimination of fatigue. *(continued on page 19)*

Predicting the Outcome of Femoral Head Osteonecrosis

Gregory C. Gardner, M.D.
Andrew Holman, M.D.
Michael Richardson, M.D.
Peter Simkin, M.D.

Osteonecrosis literally means death of bone and is seen in a variety of orthopaedic and medical settings. One of the most common causes of osteonecrosis is trauma, particularly after fracture abuse. Of the nontraumatic causes of osteonecrosis, corticosteroid therapy and alcohol abuse head the list. One of the larger categories in this nontraumatic list is "idiopathic." In 3,000 Japanese patients evaluated for nontraumatic causes of osteonecrosis, 37% had no identifiable cause.

It is estimated that 10% of the 500,000 total joint replacements done annually in the United States are for sequelae of osteonecrosis. In addition, most persons affected by osteonecrosis are young and must live with the consequences for a long time.

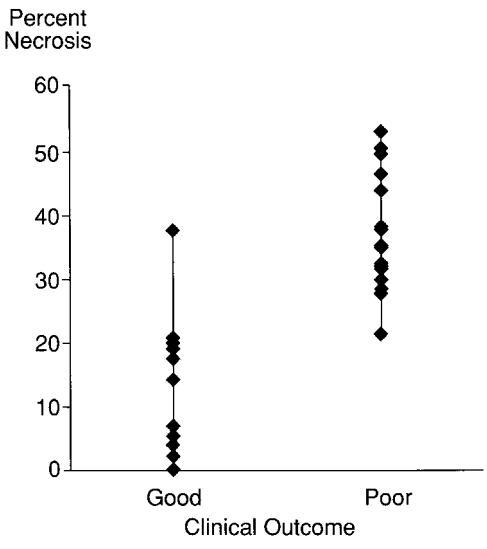

FIGURE 1: Percent femoral head necrosis by clinical outcome.

The treatment of established osteonecrosis of the femoral head has centered around the use of core decompression (CD), but the reported long-term results of CD have been quite divergent, with much debate in the literature as to its utility. Earlier CD studies relied on the Ficat radiographic stage to determine which patients were appropriate candidates for core decompression. Magnetic resonance imaging (MRI) has made it possible to diagnosis osteonecrosis even before radiographic changes are evident and also provides information on the extent of bone necrosis. It makes intuitive sense that the extent of femoral head involvement by osteonecrosis would be of prognostic importance, but until recently, this important question remained unasked.

Methods

Our team conducted a retrospective evaluation of 23 patients and 31 hips affected by osteonecrosis and treated with CD between 1986 and 1989 at the University of Washington. Corticosteroid use was the most common risk factor followed by alcohol overuse. One patient, a scuba diver, had dysbaric osteonecrosis.

We sought to determine whether measuring the volume of femoral head necrosis would predict the outcome following CD. Criteria for inclusion in the study were an MRI of the study hip within six weeks before CD, and also that the study hip be Ficat stage I or II on plain radiographs (Table I). We evaluated clinical outcome of the patients prior to examining the MRI scans. A good outcome was defined as pain reduction and no planned or completed total hip arthroplasty (THA), while a poor outcome was considered worse pain and/or THA planned or accomplished at follow-up.

We analyzed the preoperative MRI scan by first digitizing the images onto a Macintosh computer, then measuring the area of necrosis of each available MRI slice using a NIH shareware program called Image. The area of necrosis was compared to the total area of the femoral head on the MRI slice. The sum of the infarcted areas from all available MRI slices (average 4.7 slices per hip) divided by the sum of the total femoral head areas gave us an excellent estimate of the percent volume of femoral head necrosis (Figure 1). Interobserver variation in measurement was less than 3%.

Results

Fifteen hips had a good outcome as defined above and 16 had a poor outcome. The good outcome group had a mean follow-up of 32 months (range 18-67 months) and a mean age of 37 years. Fourteen of the 16 hips with a poor outcome underwent THA or had a THA planned a mean of 17 months post-CD (range 6-36 months). The remaining two hips did not have planned hip surgery because the patient died or had a serious medical illness. Mean age of the poor outcome group was 41 years.

Follow-up radiographs were available for 10 of 15 good outcome hips and none showed any further progression. Ten of 16 poor outcome hips also had post-CD follow-up radiographs and all demonstrated progression in Ficat stage.

TABLE 1: Ficat Radiographic Classification of Femoral Head Osteonecrosis

Stage	Appearance
I	Normal radiographic appearance of the femoral head
IIA	Sclerosis, osteopenia, and cystic changes
IIB	Appearance of subchondral fracture
III	Loss of sphericity and flattening of the femoral head
IV	Secondary degenerative changes

Eight of the 10 advanced to stage III and the other two went from stage I and IIA to stage IIB (evidence of subchondral fracture).

The percent volume of necrosis for the 31 study hips ranged from 0-52.6%. The patient with 0% necrosis had histologic evidence of osteonecrosis on CD histologic specimen. Percent necrosis in the good outcome group ranged from 0-37.4% (mean 12.5 +/- 2.7% SE), while those in the poor outcome group ranged from 21.6 to 52.6% (mean 37 +/- 2.3% SE) (Figure 2). Only one subject with greater than 21% necrosis met our criteria for good outcome. This patient had 37.4% necrosis of the left femoral head and reported improvement in pain post-CD but was wheelchair bound and on narcotic medications due to pain from severe right femoral head osteonecrosis. He could not be considered for THA of either hip due to severe alcoholic liver disease.

Analysis demonstrated that measurement of the preoperative percent volume of necrosis of the femoral head was highly predictive of clinical outcome. Neither Ficat stage (I vs II), risk factors for osteonecrosis, nor preoperative pain scores correlated with outcome.

Discussion

These results demonstrate the clinical usefulness of measuring the extent of femoral head necrosis prior to considering CD for treatment of osteonecrosis. They suggest that CD in hips with more than 21% of femoral head involvement may be unnecessary because progression continues despite the procedure. Whether it is useful for hips with less than 21% involvement is not answered by this study, although recent evidence from Lafforgue and co-workers suggests that small osteonecrotic hip lesions do not progress even without CD.

In addition, within the last year, reports from Lafforgue, Takatori, and others indicate that the size of the osteonecrotic lesion influences progression, which strengthens our findings.

In summary, our data and those from other centers suggest that extent of necrosis, and not core decompression, affects the progression of osteonecrosis. Previous outcome studies using CD for the treatment of femoral head osteonecrosis need to be interpreted in this light.

Recommended Reading

Lafforgue P, Dahan E, Chagnaud C, et al: Early-stage avascular necrosis of the femoral head: MR imaging for prognosis in 31 cases with at least 2 years of follow-up. *Radiology*, 187:199-204, 1993.

Mankin HJ: Nontraumatic necrosis of bone (osteonecrosis). *N Eng J Med*, 326:1473-1479, 1992.

Simkin PA, Gardner GC: Osteonecrosis: Pathogenesis and practicalities. *Hosp Practice*, 29(3): 73-84, 1993.

Simkin PA, Downey DJ: Hypothesis: retrograde embolization of marrow fat may cause osteonecrosis. *J Rheumatol*, 14:870-872, 1987.

Takatori Y, Kokubo T, Ninomiya S, et al: Avascular necrosis of the femoral head: Natural history and magnetic resonance imaging. *J Bone Joint Surg*, 75-B:217-221, 1993.

Wang GJ, Sweet DE, Reger SI, et al: Fat-cell changes as a mechanism of avascular necrosis of the femoral head in cortisone-treated rabbits. *J Bone Joint Surg*, 59-A:729-735, 1977.

AO Fracture Classification Consistency for the Distal Radius

Hans J. Kreder, M.D.
Douglas P. Hanel, M.D.
Marc F. Swiontkowski, M.D.

Variables that affect the outcome being measured, independent of the intervention or exposure of interest, are known as potential confounding factors. When they are distributed unevenly across patient populations being compared, conclusions may be biased unless the confounding factors are controlled.

Dorey has urged researchers to present their results stratified by important risk factors such as age and disease etiology. Ideally, these confounding factors are controlled by randomly assigning treatment, or by carefully adjusting for these variables using statistical techniques. Even in prospective studies, major confounding factors must be considered in describing and communicating information about the patient population under investigation, and also to gain a deeper understanding of the interplay between the particular factor, treatment, and ultimate functional outcome.

Injury severity represents one potential confounding factor that is likely to affect patient outcome, although other variables such as patient age, socioeconomic status, and comorbidity may be more important. The AO classification of fractures represents an attempt to provide a measure of injury severity, with higher grades indicating more severe fractures with a worse prognosis. Inter and intra-observer consistency is a prerequisite for the effective use of any fracture severity classification system if it is to be used for risk stratification.

Our study sought to: (1) quantify agreement in applying the AO classification to distal radius fractures, (2) quantify agreement in recognizing articular displacement, (3) evaluate clinician responses regarding anticipated prognosis and suggested treatment, (4) investigate factors that might improve rater consistency.

Methods

We selected 36 patient records at random from our trauma database containing information on most fractures seen at Harborview Medical Center over the last five years, including a record of the AO classification (usually assigned by the house staff on patient admission). Four patients were chosen from each of the nine possible assigned AO "groups." For three of these patients, preoperative films were not available and these patients were excluded.

An independent radiologist graded the presenting anteroposterior (AP) and lateral films of the remaining 33 patients as to adequacy of joint and fracture visualization, with attention to orthogonality of the two views, visualization of Guilula's arc on the AP, visualization of the proximal lunate cortex on the lateral, dislocation of the carpus, presence of artifact, evidence of prior trauma, and partial healing of the fracture (i.e., if the patient delayed seeking medical care).

After a review of the AO classification system specific to the distal radius, a group of 8 consultants, 9 fellows, 15 residents, and 4 nonclinicians from three centers were asked to classify each fracture with the aid of a handout illustrating all 27 AO fracture subgroups. Furthermore, each rater was asked whether the articular surface was incongruous (displaced) or congruous (no detectable displacement). Finally, the raters were asked to choose from among four treatment possibilities (casting, percutaneous/external fixation, limited open/indirect reduction, open reduction with internal fixation), and to estimate the ultimate prognosis.

Raters were given standard patient demographics, which were identical for all 33 patients. The standardized treatment options and prognosis criteria had also been explained prior to grading. The same radiographs were then reclassified two to four weeks later. Because some fractures will be graded the same purely by chance, it is necessary to use a statistic that adjusts for the amount of coincidental agreement. The SAV statistic of O'Connell and Dobson was used in this study. It allows computation of chance-adjusted rater agreement for multiple raters analogous to the multiple-rater kappa statistic. The statistical values can range from a high of 1, representing perfect agreement on every case, to -1, representing complete disagreement on every case. An SAV value of 0 suggests that the observed agreement is purely explainable by chance alone.

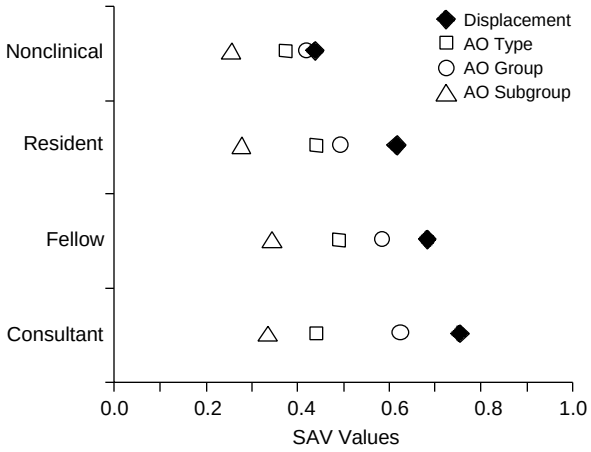

FIGURE 1: Interobserver Agreement: SAV values are plotted by rater experience and increasing complexity of the AO classification from three types to nine groups and 27 subgroups. The last classification category represents rater agreement regarding articular surface displacement. The SAV statistic is a measure of agreement that is corrected for chance agreement among multiple observers. A value of 1 represents complete agreement beyond chance. The plotted values are unweighted (i.e., no partial credit is given for adjacent responses).

Koch and Landis have outlined some admittedly arbitrary but widely quoted criteria for the interpretation of chance-corrected agreement. Values between .0 and .2 represent slight agreement, .21 and .4 fair agreement, .41 and .6 moderate, .61 to .8 substantial agreement, and above .81 is considered almost perfect agreement. Agreement was stratified by clini-cian experience for each outcome of interest.

Results

Three of 36 raters (two consultants and one fellow) indicated that they regularly use the AO classification system for the distal radius, while 23 raters indicated familiarity with the classification. Eighteen raters regularly used the Frykmann classification and six employed the universal system or a modification, while 12 others did not regularly apply any classification system for distal radius fractures.

AO Categories

Inter-rater agreement decreased with expansion of the classification system from three types to nine groups and 27 subgroups (Figure 1). In general, interobserver agreement improved with increasing rater experience; however, this trend decreased when the classification was expanded to the full 27 categories. Thus, the attending traumatologists were just as likely to disagree on the specific subgroup as were the non-clinicians. Inter-rater agreement among those clinicians who indicated prior familiarity or use of the AO classification was no better than clinicians without such experience. The highest level of agreement was observed among attending traumatologists with SAV values of .63 for the AO type, .44 for the nine possible groups, and .32 for the 27 subgroups.

Articular Displacement

Agreement was substantial for articular surface status (Figure 1). For some radiographs with high agreement for joint displacement, raters demonstrated major disagreement regarding the AO classification (Figure 2). In general, agreement was higher for joint displacement as compared with AO type after adjusting for rater experience.

Treatment and Prognosis

Clinician interobserver agreement regarding suggested fracture treatment was slight to fair (SAV was .2 for residents, .28 for fellows, and .26 for consultants). The expected prognosis was agreed upon with SAV values of .34 for residents, .45 for fellows, and .43 for consultants.

Choice of treatment correlated most strongly with assigned joint status. Open procedures and limited open procedures were more likely to be selected when the joint was classified as incongruous. The expected prognosis also correlated most closely with the assigned joint status. When articular displacement status for the same fracture was changed

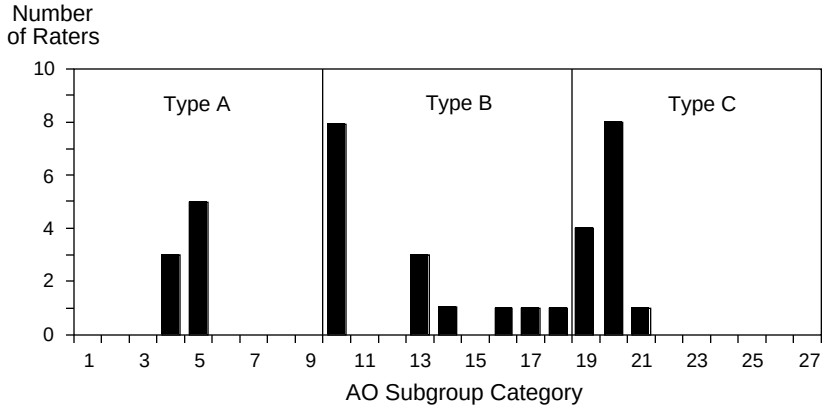

FIGURE 2: X-Ray Number Five Ratings: Interobserver agreement regarding the AO classification for this particular radiograph was low. When asked to categorize the joint surface as either displaced (any detectable step displacement) or undisplaced, raters were in much better agreement, with 81% of the 36 raters classifying the joint as undisplaced (SAV = .6).

at the second rating, the new treatment choice was likely to reflect the most recently assigned joint status; how-ever, prognosis was less likely to be altered from the initially assigned value. Similarly, when the AO type was changed from one time to the next, the expected prognosis was not likely to change; however, suggested treat-ment often reflected the new AO type. Residents were more likely to correlate treatment with the AO classification than were fellows or consultants.

Radiographic Variables

Healing fractures were subject to the most significant disagreement. When all three such films were removed from the analysis, the level of agreement rose by 5-10% for all participants in most rating categories. Less significant effects were noted for the other radiographic variables mentioned above.

Intraobserver Consistency

Intraobserver SAV values were highest for the variable "articular displacement" (.40 for nonclinicians to .82 for fellows and consultants). Consistency decreased with expansion of the classification to 27 subgroups so that intraobserver agreement was only fair for the specific type-group-subgroup combination, with substantial agreement for the type alone. In general, nonclinicians were the least consistent, while consultants agreed with themselves most often.

Discussion

The AO fracture classification system involves three sequential decisions regarding specific fracture characteristics. At each step in the decision-making process, disagreement can arise such that confusion regarding the precise designation into one of 27 possible categories is extremely high. Raters were much more likely to agree as to whether or not the joint was displaced than on the precise nature of the fracture lines that must be identified to apply the complete AO classification. Only at the first decision step (categorizing the fracture as type A, B or C; extra-articular, partial, or complete articular) did the most experienced raters demonstrate substantial agreement among themselves.

The severity of the specific fracture in question represents one of many important variables that must be considered when comparing the results of nonrandomized studies. The AO system allows collapse down to three "types" for stratification by injury severity, with the possibility of expansion for what was hoped would provide more detailed fracture pattern information that might be useful in planning treatment. This is an attractive concept in theory, but for distal radius fractures there is no prospective research to suggest that outcome varies with the classification or that each of the expanded 27 subgroups correlates with important treatment considerations.

In general, we feel that treatment should be based upon sound basic principles of fracture care and anatomy as well as a consideration of the specific patient and institutional circumstances, rather than relying on a specific fracture classification system. Our main interest, therefore, is the consideration of a classification for the purpose of injury severity adjustment. For distal radius and other periarticular fractures, evidence suggests that displaced intra-articular fractures would generally be expected to have a worse prognosis than would extra-articular or undisplaced articular injuries. Thus, the presence or absence of initial articular displacement should be included in any classification that is intended to reflect injury severity, although good prospective data is lacking regarding this point.

Because articular status is the most consistent measure among all experience groups, it may be that categorizing fractures into articular displaced versus articular nondisplaced is sufficient for nonresearch purposes. Unfortunately, the AO classification does not consider fracture displacement at all for defining fracture types, groups, or subgroups. Given the confusion in applying the classification for the more detailed AO groups and subgroups, these categories are of little use for risk adjustment.

When classifying fractures for research purposes, stratifying by displacement status of the articular surface (displaced or undisplaced) a well as the AO type should be considered. These two variables should be graded by experienced clinicians, as both interobserver and intraobserver consistency improve with rater experience. Ideally, a consensus of such raters should be sought. No attempt should be made to classify healing fractures because radiographs of such injuries cannot be accurately interpreted. AO type and articular displacement are consistent measures when classification is done by experienced raters, but prospective research is needed to demonstrate the utility of these measures in predicting patient-oriented functional outcome.

Recommended Reading

Dorey F, Grigoris P, Amstutz H: Editorial: Making do without randomized trials. *J Bone Joint Surg*, 76B(1):1-3, 1994.

Posner KL, Sampson PD, Caplan RA et al: Measuring inter-rater reliability among multiple raters: An example of methods for nominal data. *Stat Med*, 9:1103-1115, 1990.

Trumble TE, Schmitt SR, Vedder NB Factors affecting the functional outcome of displaced intra-articular distal radius fractures. *J Hand Surg*, 19A(2):325-340, 1994.

Primitive Neuroectodermal Tumor and Extraskeletal Ewing's Sarcoma: A Comparison of Clinical Features and Management

James D. Bruckner, M.D.
Ernest U. Conrad III, M.D.
Carolyn Collins, M.D.
Rodney A. Schmidt, M.D.
Denis R. Benjamin, M.D.
Leslie S. Malo, M.D.

Primitive neuroectodermal tumors (PNET) are undifferentiated, small, round-cell tumors that occur principally in the soft tissues. Ewing's sarcoma is also an undifferentiated, small, round-cell tumor originally thought to occur exclusively in bone. While the histogenesis of Ewing's tumor has been debated for years, it is now generally accepted that it arises from a mesenchymal stem cell of neural crest origin.

In 1975, Angervall and Enzinger first described 39 cases of Ewing's sarcoma of the soft tissues. Subsequent reports of similar tumors loosely referred to these lesions as extraskeletal Ewing's sarcoma (EES). Recent ultrastructural and immunohistochemical studies, and the existence of a common gene rearrangement, suggest that EES and PNET are soft-tissue tumors with a common histogenesis. Protooncogene expression in PNET is also identical to that of Ewing's sarcoma, suggesting that these tumors may share important biologic features that affect their clinical behavior. If true, it would be reasonable to postulate that PNET and EES should respond similarly to the same treatment regimens.

Our review retrospectively examined and compared the clinical characteristics and response to treatment of previously diagnosed primitive neuroectodermal tumors and extraskeletal Ewing's sarcomas treated at our institution.

TABLE 1: Comparison of Primitive Neuroectodermal Tumors (PNET) and Extraskeletal Ewing's Sarcoma (EES).

	PNET	EES	Total
Age			
Average (years)	16	20	17.7
Number > 18	6	7	13
Number ≤ 18	8	3	11
Gender			
Male	9	8	17
Female	5	2	7
Location			
Extremity	4	4	8
Chest wall/thorax	3	2	5
Paraspinal	1	2	3
Head and neck	3	1	4
Abdominal	2	1	3
Pelvic	1	0	1
Stage			
IIIA	3	0	3
IIIB	9	8	17
IVA	1	0	1
IVB	1	2	3
End Result			
Alive, no evidence of disease	5	4	9
Dead of disease	8	6	14
Alive, with disease	1	0	1

Methods

We retrospectively reviewed the cases of all patients diagnosed with PNET and EES between 1968 and 1990 at the University of Washington Medical Center and Children's Hospital and Medical Center. Routine demographic data, location and stage of the lesion, presenting symptoms, and treatment modalities employed in each case were recorded, including the type of chemotherapy (if any), the amount of radiation used (if any), and the number and type of surgical procedures performed. Disease-free survival periods were determined for each patient, based on local recurrence and distant metastasis. Length of follow-up was calculated using a patient's last recorded clinic visit or the date of death.

Results

Twenty-four cases met criteria for inclusion in this study. Fourteen were diagnosed as PNETs and 10 were EESs. Table 1 gives comparison data for the two groups.

TABLE 2: Results of Treatment According to Treatment Rationale (Stage III Patients)

Treatment	Number of Patients	Disease Free (%)	Dead of Disease (%)	Average EFI* (months)	Average Follow-up (months)
A	10	3 (30)	7 (70)	18	40
B	7	6 (86)	1 (14)	27	33

*Event Free Interval = average of time to metastasis or local recurrence.

The mean follow-up for both groups was 33 months (range 1-131 months). Ten of the 24 patients (42%) were alive at the most recent follow-up. Nine (37%) were continuously disease free at a mean follow-up of 43 months. Follow-up averaged 44 months in those patients with EES (range 1-131 months), and 25 months in those patients with a PNET (range 8-69 months). The survival for patients with a PNET was six of 14 or 43%, for patients with a EES it was four of 10 or 40%. The disease free survival (DFS) for PNET is five of 14 or 36%. Of the patients who are currently considered disease free, five (56%) had a PNET and four (44%) an EES.

Twenty patients had nonmetastatic (stage III) disease and four had metastatic disease (stage IV). Of the four stage IV patients, three died of their disease at a mean of 14 months (range 1-26 months) after presentation. At the time of this writing, one stage IV patient is alive with evidence of progressive disease 19 months after diagnosis.

The therapeutic approach varied in the 20 patients with localized disease. All but three received either preoperative or postoperative adjuvant chemotherapy combined with surgery and radiation therapy. The three patients who did not receive early adjuvant chemotherapy died of recurrent local disease or metastatic disease at 15, 20, and 31 months after diagnosis.

The remaining 17 patients with localized disease fell into two groups. Group A patients had an incisional or excisional biopsy without any attempt at wide resection, followed by adjuvant chemotherapy and radiation therapy. Group B patients had a biopsy followed either immediately or after induction chemotherapy by a wide local resection. Adjuvant chemotherapy was then continued postoperatively, combined with radiation therapy. A comparison of treatment results in these two groups is shown in Table 2. Survival data comparing PNET and EES by treatment rationale and diagnosis is shown in Table 3. Eighty-six percent of patients who had a wide local or radical resection of their tumor (group B) as part of their treatment are disease free at an average of 33 months follow-up (five PNET and two EES). Thirty percent of those who did not have a wide or radical resection (group A) are disease free at an average of 40 months follow-up (one PNET and two EES).

The local recurrence rate for stage III patients receiving conventional combination treatment was 35% (six of 17). Four PNETs and two EESs recurred locally. All local recurrences occurred in group A patients, who had no attempt at wide resection of their tumors. There were no local recurrences in group B patients. Late metastases (excluding the case just mentioned) occurred in five of 17 stage III patients (29%). Four of five late metastases occurred in group A patients at an average of 25 months after diagnosis (range 2-75 months). Three developed widespread skeletal metastasis and the fourth, pulmonary metastasis. Three of five late metastases were PNETs and two of five were EES. One group B patient had metastasis to regional lymph nodes 11 months after treatment of a submaxillary primary tumor. He is free of disease at 34 months following radical lymph node resection.

TABLE 3: Survival by Treatment Rationale and Diagnosis

	Number of Patients	Disease Free (%)	Dead of Disease (%)
Treatment Group A			
PNET	5	1 (20)	4 (80)
EES	5	2 (40)	3 (60)
Treatment Group B			
PNET	5	4 (80)	1 (20)
EES	2	2 (100)	0

Discussion

Our ability to make any significant observations regarding these unusual tumors is based on the reliability of our diagnostic criteria. While histologic subtypes have not been recognized as a major determinant of treatment results for most sarcomas, it is extremely important to continue efforts to define biologic differences in different sarcomas to refine their diagnosis and the assessment of treatment results. Poor risk categories cannot be addressed if they cannot be identified.

In this study, 10 patients had the diagnosis of extraskeletal Ewing's sarcoma, and 14 had the diagnosis of peripheral neuroectodermal tumor. In all cases, the diagnosis was based upon conventional histopathologic criteria. Theoretically, because these lesions arise from a common neuroepithelial progenitor cell, they should behave in a similar fashion clinically and respond to similar treatment methods. However, there is no series in the literature that compares the response of these two tumors to treatment. Our data suggest that EES responds better to treatment than does PNET, with fewer local recurrences and late metastases, and longer disease-free survival.

The evidence for the effectiveness of neoadjuvant chemotherapy in preventing locally persistent disease and widespread metastasis appears to be enlarging as our experience grows with these unusual tumors. While most current series examining the clinical behavior of both PNETs and EESs suggest that treatment should consist of aggressive combined modality regimens employing combination chemotherapy, surgery, and radiation therapy, the issue of the timing and extent of surgery remains unanswered.

We were able to identify two different treatment approaches in this group of patients. The first (group A) employed adjuvant chemotherapy and radiation therapy after incisional or excisional biopsy. Results in this group, as expected, were poor, with 30% of patients free of disease at an average of 40 months after surgery. The second treatment approach (group B) used a biopsy followed by a wide local resection or amputation, either immediately or after a variable period of neoadjuvant chemotherapy. Chemotherapy was continued postoperatively in this group and radiation therapy used to augment local control. With this treatment, 80% of patients with PNET and 100% of patients with EES are disease free at 33 months follow-up. These data suggest that more aggressive surgical intervention is justified.

In conclusion, an enlarging body of literature points to a common neuroepithelial cell of origin for EES and PNET. Our review suggests that optimal treatment of these lesions should include an incisional biopsy, with care taken to obtain adequate specimen for immunohistochemical, ultrastructural, and cytogenetic study, followed by combination chemotherapy. A wide local or radical surgical resection or amputation should then be performed, followed by additional chemotherapy. Local radiation may be added to this regimen to improve local disease control in cases of marginal, contaminated, or unresectable surgical lesions.

Recommended Reading

Angervall L, Enzinger RM: Extraskeletal neoplasm resembling Ewing's sarcoma. *Cancer,* 36:240-251, 1975.

Hashimoto H, Enjoji M, Nakajima T, et al: Malignant neuroepithelial (peripheral neuroblastoma): A clinicopathologic study of 15 cases. *Am J Surg Pathol,* 7:309-318, 1983.

Jürgens H, Bier V, Harms D, et al: Malignant peripheral neuroectodermal tumors. *Cancer,* 61:349-357, 1988.

Marina NM, Elcubanas E, Parham DM, et al. Peripheral primitive neuroectodermal tumor (peripheral neuropepithelioma) in children. *Cancer,* 64:1952-1960, 1989.

Schmidt D, Herrmann C, Jürgens H, Harms D: Malignant peripheral neuroectodermal tumor and its necessary distinction from Ewing's sarcoma. *Cancer,* 68:2251-2259, 1991.

Fatigue (from page 11)

Recommended Reading

Belza B: Comparison of self-reported fatigue in rheumatoid arthritis and controls. *J Rheumatol* (in press).

Belza B, Henke C, Yelin E, et al: Correlates of fatigue in older adults with rheumatoid arthritis. *Nursing Res,* 42:93-99, 1993.

Chen M: The epidemiology of self-perceived fatigue among adults. *Prev Med,* 15:74-81, 1986.

Gerber L: Exercise and arthritis. *Bull Rheum Dis,* 39(6):1-9, 1990.

Kirk J, Douglass R, Nelson E, et al: Chief complaint of fatigue: A prospective study. *J Fam Prac,* 30:33-41, 1990.

Kroenke K, Wood D, Mangelsdorff D, et al: Chronic fatigue in primary care: Prevalence, patient characteristics, and outcome. *JAMA,* 260 (7):929-934, 1988.

Lewis S, Haller R: Physiologic measurement of exercise and fatigue with special reference to chronic fatigue syndrome. *Rev Infec Dis,* 12 (suppl 1):S98-108, 1991.

Pinals R, Masi A, Larsen R: Preliminary criteria for clinical remission in rheumatoid arthritis. *Arth Rheum,* 24:1308-1315, 1981.

Potempa K: Chronic fatigue. *Ann Rev Nurs Res,* 11:57-76, 1993.

Posterior Instrumentation of the Unstable Cervicothoracic Spine

Jens R. Chapman, M.D.
Paul A. Anderson, M.D.

Fractures of the cervicothoracic junction pose a diagnostic and therapeutic challenge. The region is difficult to image with plain radiography and difficult to immobilize with external orthoses because of biomechanical forces in this transitional portion of the spinal column. Recently, several internal fixation techniques have been developed for stabilization of cervical fractures and dislocations. This study reports our experience with AO reconstruction plates at the cervicothoracic junction in 23 patients. Specifically, we examined the effects of surgery regarding neurologic deficit, spine stability, maintenance of alignment, and complications.

Methods

This prospective study is based on the charts and radiologic records of 23 consecutive patients with cervicothoracic instability, defined as pathology involving the vertebral segments C7 through T2, who were treated at the University of Washington's Harborview Medical Center. The patients ranged in age from 27 to 73 years (average, 47 years). Fifteen patients were men and eight were women.

Neurologic examination revealed great diversity in this population. Four were neurologically intact, six were complete quadriplegics and 12 incomplete quadriplegics, of whom five had focal cervical radiculopathies. One patient was paraplegic. The neurologic deficits were scaled according to Frankel.

Radiologic studies for all patients revealed unstable spines; 19 patients had fractures or ligamentous instabilities due to trauma, two due to neoplastic processes, and two due to ankylosing spondylitis. Twelve patients were involved in motor vehicle accidents with acute onset of instability. Four patients were injured in falls, two were struck by falling trees while logging, and two had ankylosing spondylitis. One patient was involved in a car versus bike accident. Two patients had instability from tumors of the vertebral column.

All patients were treated by posterior cervical arthrodesis using AO reconstruction plates and autogenous iliac bone graft according to the technique of Anderson and Grady. Following assessment of the patient clinically and radiographically, closed reduction of the spinal column was achieved expeditiously with skeletal traction. Operative stabilization was performed between three and seven days after admission for patients with acute injury. AO reconstruction plates with an 8- or 12-mm hole spacing were contoured to fit the normal curvature of the cervicothoracic region. Screws of 16 to 18 mm in length were placed in the lateral masses of the cervical spine. The lateral mass in the thoracic spine evolves to a transverse process insufficiently strong for screw fixation. Therefore, below C7, screws 16 to 22 mm in length were placed in the pedicles. Interspinous wiring was used in those patients with intact spinous processes. Postoperative immobilization consisted of bracing for two months.

Results

Follow-up averaged 22 months for surviving patients (range 12 to 54 months). Two patients died at two and four months after surgery secondary to respiratory compromise. Another patient died accidentally from carbon monoxide poisoning 18 months after surgery.

Follow-up examination revealed that no patient's neurologic status deteriorated as a result of the surgery (Table 1). All four patients who were intact before the surgery remained intact at follow-up (Frankel E). All incomplete quadriplegics improved at least one Frankel level. All patients with Frankel D incomplete quadriplegia and those with cervical radiculopathies returned to normal following surgery. Of the four patients with Frankel C incomplete quadriplegia, two improved to Frankel D, and two improved to Frankel E. Of the seven patients with complete quadriplegia (Frankel A), five were unchanged, one improved to Frankel B, and one to Frankel C.

TABLE 1: Neurologic Outcome According to the Frankel Scale for 25 Patients with an Average Follow-up of 15.4 months

Preoperative Frankel Level	Postoperative Frankel Level A	B	C	D	E
A = 7	5	1	1		
B = 1				1	
C = 4				2	2
D = 7					7
E = 4					4

A = complete loss of motor and sensory function
B = preservation of sensory function, not motor
C = motor useless
D = motor incomplete
E = normal motor and sensory function

Fracture types were equally variable. Six patients had vertebral body burst fractures, five at C7 and one at T2. Five patients had unilateral or bilateral facet fracture-dislocations, three patients had pure dislocations, and five had multiple-element fractures at two to five levels. In two patients, instability was the result of previous accidents and spine procedures. Two patients had metastatic lesions of the vertebral bodies of C7 and / or T1.

The number of motion segments fused ranged from two to 12 with an average of four. Treatment of the burst fractures usually necessitated two or three levels of fusion; however, two cases with additional ligamentous injuries required more — five levels for one and nine for another. Typically, adequate stability was achieved for the fracture-dislocations by fusing only two or three segments. Pure dislocations required three to four levels of fusion. The patients with multilevel injuries were successfully treated with three to six motion segments fused. The patients with instability due to previous spinal procedures and the patients with the metastatic lesions required five to seven motion segments of fusion.

All patients had solid arthrodeses based on flexion-extension radiographs. An increase in kyphosis past the vertical plane did not occur in any patients. One patient with previous cervical fusion had increased translational displacement of 0-3 mm. Radiographs showed that the patient fused solidly and experienced no postoperative complications.

One patient reported mild pain at follow-up, while two patients reported significant pain. This procedure caused no vascular or pulmonary complications. In one patient, two screws loosened with no associated problems; flexion-extension radiographs revealed solid arthrodesis. Wound dehiscence with no evidence of infection occurred in one patient three weeks postoperative; the wound healed after extensive debridement and pulsatile lavage.

Discussion

Diagnosis and treatment of the unstable cervicothoracic junction is particularly problematic for several reasons. Lateral radiographs of the cervical spine often fail to show the anatomy at this junction. Treatment of cervicothoracic injuries is challenging because of significant biomechanical forces at this portion of the spinal column. The lordotic and highly mobile cervical spine connects with the kyphotic and relatively immobile thoracic spine resulting in a region that is structurally and physiologically precarious.

Past treatment of cervicothoracic fractures has included external orthoses and immobilization with limited success. The halo fixation device is the most commonly used device to immobilize the unstable cervical spine and provides more rigid immobilization compared with other orthoses. However, failure of immobilization in the lower cervical spine is well documented in the literature, presumably owing to residual mobility at individual segments of the unstable spine.

According to many authors, surgical treatment aimed at immediate stability is appealing because it provides an increased incidence of spinal stability and permits early mobilization and muscle strengthening, which reduces the physical and psychological morbidity resulting from prolonged recumbency. Anterior surgical reconstruction and instrumentation of the cervicothoracic junction has the advantage of allowing for decompression of the spinal cord and restoration of the load-bearing anterior spinal column. However, the rib cage hinders accessibility of this area of the spine, limiting the ability to place ventral stabilizing instrumentation.

Posterior stabilization techniques have the advantage of a simple approach and provide the possibility of multilevel segmental fixation on the tension side of the spinal column. Bony fusion provided long-term stability. With intact spinous processes and lamina, posterior wiring with autogenous bone graft has shown excellent results. Limitations exist with this technique, particularly in patients with multilevel injuries, absent or deficient facets, spinous processes, and laminas, or with extension and rotational instabilities.

Conventional rod and hook constructs have limited applicability in the lower cervical spine due to the small size of the vertebral bone structures, the small spinal canal dimensions, and the relatively large spinal cord. Sublaminar wires pose a considerable risk to neural structures in the lower cervical spine.

Anderson and several other authors have reported fusion rates ranging from 95% to 100% using posterior plating of the cervical spine with autogenous iliac crest bone grafting. Posterior plating of the cervicothoracic junction requires a variation in the site of screw placement from previously described techniques. In the cervical spine screws are placed in the lateral masses, but in the thoracic spine the lateral masses evolve into the transverse processes, which are insufficiently strong for screw placement. For that reason, below T1, screws are placed in the pedicles.

Posterior lateral mass plating with AO reconstruction plates and autogenous iliac bone graft has been a successful method of treatment for fractures of the cervicothoracic junction based on the parameters of our investigation. No patient's neurologic status deteriorated as a result of the procedure, and 70% showed an improvement of at least one Frankel level. All patients had solid arthrodeses based on flexion-extension radiographs. Only one patient experienced an increase in deformity, 3 mm of displacement, which was not clinically significant. Complications from the surgery were minimal. No vascular or pulmonary accidents occurred. Only 13% of the patients experienced pain. In summary, posterior arthrodesis using AO 2.7- and 3.5-mm reconstruction plates and autogenous iliac bone graft is a promising method of treatment for cervicothoracic instability.

Recommended Reading

Anderson PA, Henley MB, Grady MS, Montesano PX, Winn HR: Posterior cervical arthrodesis with AO reconstruction plates and bone graft. *Spine,* 16(3S):72-79, 1991.

Birch R, Bonney G, Marshall RW: A surgical approach to the cervicothoracic spine. *J Bone Joint Surg,* 72-B(5):904-907, 1990.

Bucci MN, Dauser RX, Maynard FA, Hoff JT: Management of posttraumatic cervical spine instability: Operative fusion versus halo vest immobilization: Analysis of 49 cases. *J Trauma,* 28(7):1001-1006, 1988.

Evans DK: Dislocations at the cervicothoracic junction. *J Bone Joint Surg,* 65B(2):124-127, 1983.

Frankel HL, Hancock DO, Hyslop G et al: The value of postural reduction in the initial management of closed injuries of the spine with paraplegia and tetraplegia. *Paraplegia,* 7:1179-192, 1969.

Garfin SR, Botte MJ, Waters RL, Nickel VL: Complications in the use of the halo fixation device. *J Bone Joint Surg,* 68A:320-325, 1986.

Glaser JA, Whitehall R, Stamp WG, Jane JA: Complications associated with the halo-vest. *J Neurosurg,* 65:762-769, 1986.

Micheli LJ, Hood RW: Anterior exposure of the cervicothoracic spine using a combined cervical and thoracic approach. *J Bone Joint Surg,* 65-A(7):992-992-997, 1983.

Nichols CG, Young DH, Schiller WR Evaluation of cervicothoracic junction injury. *Ann Emerg Med,* 16:640-642, 1987.

Anterosuperior Humeral Displacement: Limitation by the Coracoacromial Arch

Mark D. Lazarus, M.D.
Douglas T. Harryman II, M.D.
Shing-Wai Yung, M.D.
John A. Sidles, Ph.D.
Frederick A. Matsen III, M.D.

The humeral head is usually stabilized against anterosuperior displacement by the dynamic action of the rotator cuff, which resists the upward pull of the deltoid. With large loads or in patients in whom the cuff is deficient, anterosuperior stability may depend on the coracoacromial arch. However, the integrity of this arch is often sacrificed in rotator cuff surgery. This study investigated the degree to which the coracoacromial arch acts as a barrier to anterosuperior humeral displacement in the cuff-deficient shoulder, and analyzed the effect of coracoacromial ligament release and anterior acromioplasty on this deterrent.

Methods

Six fresh-frozen normal glenohumeral joints from cadavers (mean age of 80 years at death, range 69 to 92 years) were prepared by resecting all muscles and tendons. The coracoacromial ligament and the glenoid labrum were left intact. The direction proceeding from the glenoid center to the biceps long head origin was defined as superior (0 degrees), and the anterior perpendicular to this plane was designated as anterior (90 degrees). Spatial sensors were attached to the humeral shaft and scapula and the scapula was fixed to a force transducer.

The humeral head was placed against the posterior undersurface of the acromion. Contact was maintained with the glenoid and the head was then translated anteriorly on the undersurface of the coracoacromial arch while the position of the humeral head center was tracked.

The humeral head was translated in four directions from the glenoid, anterosuperior (45 degrees), between anterosuperior and superior (22.5 degrees), superior (0 degrees), and posterosuperior (315 degrees). Contact was maintained with the glenoid rim until the overlying coracoacromial arch was encountered, at which point the head was translated laterally around the arch, tracking the position of the humeral head center during movement.

The humeral head was then placed under the most anterosuperior aspect of the coracoacromial arch. A 30-newton compressive load directed medially toward the glenoid was applied to the humeral head and a progressively increasing anterosuperior translating force was applied until either a maximum force of 50 newtons was achieved or the humeral head escaped from under the coracoacromial arch, whichever occurred first. This protocol was completed in the intact specimens, after resection of the entire coracoacromial ligament, and after anterior acromioplasty.

Results

Anteroposterior Humeral Displacement

In the intact specimen, the plot of the center of the humeral head during anterior to posterior translation under the acromion and ligament formed a true *arch.* The mean ± SD maximum superior displacement of the humeral head was 5.9 ± 2 mm. Resection of the coracoacromial ligament or anterior acromioplasty converted this arch to a triangle (Figure 1, page 24). The maximum superior humeral displacement was 10.5 ± 2.5 mm for the coracoacromial ligament resection ($p = 0.0064$), and 18.4 ± 3 mm for the acromioplasty specimens ($p < 0.0001$) (Figure 2, page 24).

Lateral Humeral Translation

The mean ± SD maximum lateral translation for each preparation in each of the four directions of testing is displayed in Figure 3. In the 22.5-degree direction, the maximum lateral translation was significantly less for the acromioplasty group as compared to the intact preparation ($p = 0.0009$).

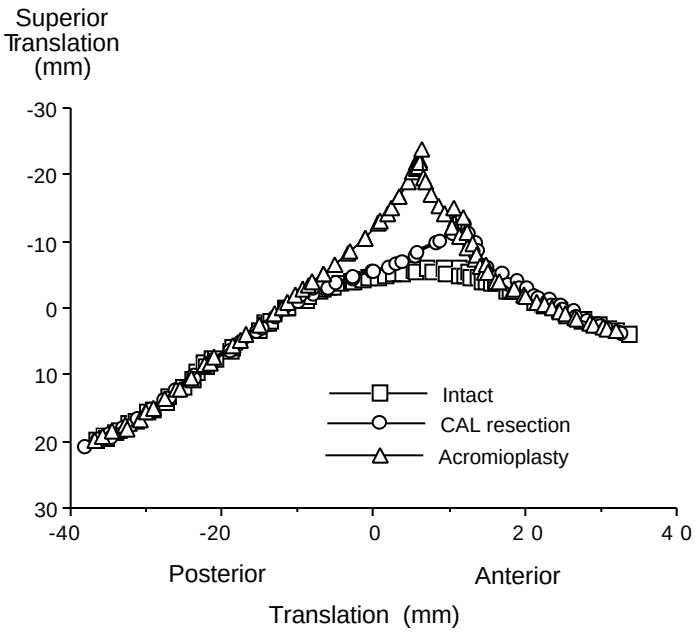

FIGURE 1: Anteroposterior humeral translation under the coracoacromial arch for a single shoulder for the intact, coracoacromial ligament (CAL) resection, and anterior acromioplasty preparations. The graph shows the change in shape after surgery on the arch.

Anterosuperior Humeral Escape

All six intact specimens maintained the humeral head beneath the coracoacromial arch up to the maximum anterosuperior translating force of 50 newtons. After anterior acromioplasty, five of six humeral heads escaped from under the coracoacromial arch at a mean translating force of 32.2 ± 9.2 newtons.

Discussion

Codman, in 1934, stated that the coracoacromial arch was an auxiliary joint of the shoulder. He felt that the roughly hemispheric shape of the arch was "almost a counterpart in size and curvature of the articular surface of the true joint." The exercises that he prescribed were designed to be performed in a stooped position so that the humeral head would not "obtain a fulcrum on the glenoid or acromion or both." He did not recommend acromioplasty during rotator cuff surgery and stated, "Evidently, the coracoacromial ligament has an important duty and should not be thoughtlessly divided at any operation."

Wiley reported on four cases of "superior dislocation" of the humeral head after anterior acromioplasty in the face of a complete rotator cuff tear. He believed that the superior location resulted from a functional loss of the coracoacromial arch. Arntz and Matsen recommended preservation of the coracoacromial arch during prosthetic humeral replacement for rotator cuff tear arthropathy, to provide "superior secondary stability" to the prosthesis. Finally, Flatow and colleagues recently advocated repair of the coracoacromial ligament after repair of a massive rotator cuff tear. They stated: "Aggressive acromioplasty in the presence of an unrepaired or nonfunctional rotator cuff can lead to anterosuperior humeral head subluxation."

We were surprised that resection of the coracoacromial ligament alone led to a significant increase in the superior displacement of the humeral head. After a routine anterior acromioplasty, the humeral head was restrained approximately 13 mm higher than in the intact specimens. Superior displacement of the head would be expected to shorten the working length of the deltoid and leave it at a mechanical disadvantage.

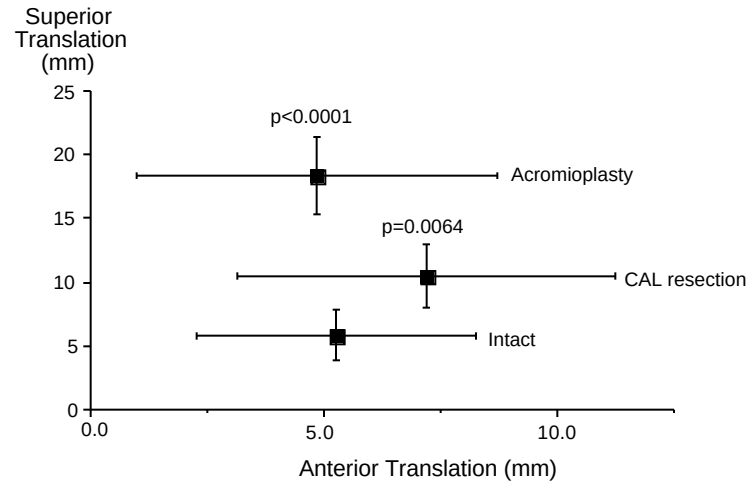

FIGURE 2: Mean ± 1SD maximum superior translation and anterior translation at the point of maximum superior translation for all six specimens for the intact, coracoacromial ligament (CAL) resection, and anterior acromioplasty preparations. Coracoacromial ligament resection and acromioplasty significantly increased superior translation (see text).

A person who wishes to scale a fence likely will choose the lowest point. Similarly, if the humeral head is going to escape from beneath the coracoacromial arch, lowering the lateral extent of the barrier will make this escape easier. In the 22.5-degree direction, the lateral extent of the coracoarcomial arch was significantly decreased after acromioplasty. Decreasing the lateral extent of the arch lessens the barrier to anterosuperior humeral escape. Hence, five of six loaded humeral heads completely escaped from the coracoacromial arch after acromioplasty and after application of an anterosuperior translating force.

In conclusion, the coracoacromial arch provides a substantial barrier against anterosuperior displacement of the humeral head in the cuff-deficient shoulder. Both resection of the coracoacromial ligament and anterior acromioplasty resulted in superior displacement of the upwardly loaded humeral head as compared to the intact condition. Standard anterior acromioplasty was associated with escape of the humeral head from under the coracoacromial arch in response to an anterosuperior translating force. These results suggest that patients in whom the normal head-centering capacity of the rotator cuff is deficient, the coracoacromial arch should be preserved to prevent major anterosuperior humeral displacement.

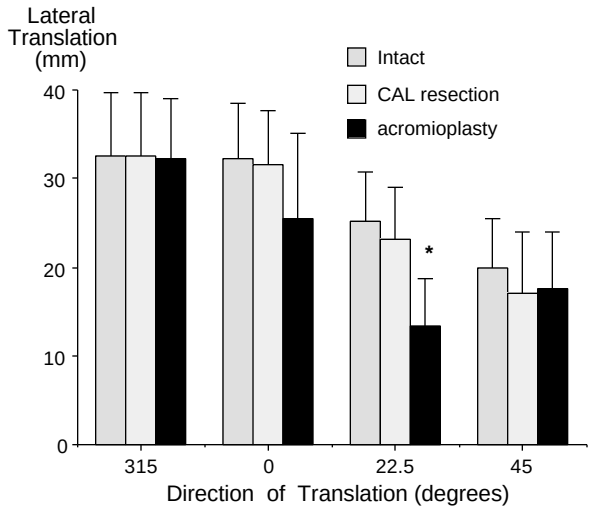

FIGURE 3: Mean ± 1SD maximum lateral humeral translation in each of the four directions for the intact, coracoacromial ligament (CAL) resection, and anterior acromioplasty preparations. *Note maximal lateral translation was significantly less for the acromioplasty group as compared to the intact preparation ($p < 0.009$).

Recommended Reading

Arntz CJ, Jackins S, Matsen FA III: Prosthetic replacement of the shoulder for the treatment of defects in the rotator cuff and the surface of the genohumeral joint. *J Bone Joint Surg*, 75A:485-491, 1994.

Burkhart SS: Fluoroscopic comparison of kinematic patterns in massive rotator cuff tears: A suspension bridge model. *Clin Orthop*, 284:144-152, 1992.

Codman EA: *The Shoulder: Rupture of the Supraspinatous Tendon and Other Lesions in or About the Subacromial Bursa.* Boston, MA: T. Todd Co., 1934.

Flatow EL, Weinstein XA, Duralde CA, et al: Coracoacromial ligament preservation in rotator cuff surgery. American Shoulder and Elbow Surgeons Annual Meeting, 1993, Williamsburg, Virginia.

Putz R, Liebermann J, Reichelt A: Funktion des ligamentum coracoacromiale. *Acta Anat*, 131:140-145, 1988.

Rockwood CA Jr, Burkhead WZ: Management of patients with massive rotator cuff defects by acromioplasty and rotator cuff debridement. *Orthop Trans*, 12:190-191, 1988.

Wiley AM: Superior humeral dislocation: A complication following decompression and debridement for rotator cuff tears. *Clin Orthop*, 263:135-141, 1991.

The "Corona Mortis" — A Cadaveric and Clinical Study

M.L. (Chip) Routt Jr., M.D.
David C. Teague, M.D.
Daniel O. Graney, M.D.

The management of displaced fractures of the acetabulum has changed over the past three decades largely due to the pioneering work of Letournel and Judet. Most acetabular surgeons recommend open anatomical reduction, rigid internal fixation, and early motion for displaced intra-articular fractures. Many operative approaches have been advocated for exposure and fixation of these fractures. The ilioinguinal, extended iliofemoral, and Kocher-Langenbeck exposures are most often recommended. The ilioinguinal approach may be unfamiliar to many orthopedists, but is becoming increasingly popular.

The retropubic vascular systems must be addressed carefully during this exposure. Letournel describes an inconstant communication between the external iliac or deep inferior epigastric arteries and the obturator artery. This anomalous anastomosis, referred to by Letournel as the "corona mortis," is reported in 10-15% of these approaches. Our study investigated the details of the retropubic vascular anatomy to better understand the systems likely to be encountered during the ilioinguinal approach.

Methods

Cadaveric Studies

We performed bilateral ilioinguinal exposures on 40 cadavers. The right side of one specimen was excluded due to unilateral pelvic anatomical destruction at the time of preparation. The retropubic vascular anatomy of each side was carefully dissected. All vessels greater than 2 mm in diameter, connecting the obturator system with a more superficial system, were identified and their courses recorded.

Clinical Studies

We also performed a prospective clinical study. Thirty-eight consecutive patients with displaced acetabular fractures were treated surgically using ilioinguinal exposures. The operations were all performed by the same surgeon (MLR). The average age of the 30 men and eight women patients was 31 years (range 13 to 67 years). A displaced both column fracture was present in 16 patients, and a displaced "T-type" fracture pattern was noted in 10. Other displaced patterns selected for open reduction using the ilioinguinal approach included seven transverse fractures, two anterior column fractures, and three anterior column posterior hemitransverse fractures.

Vascular communications between the obturator and external iliac or inferior epigastric systems along the posterior aspect of the superior pubic ramus were identified and controlled with metallic vascular clips. These vascular clips were easily visible on the postoperative radiographs. Intraoperative blood loss was recorded. Obturator nerve function was assessed postoperatively by physical examination for each patient.

Results

Cadaveric Studies

Venous anastomoses were common. Forty-seven of 79 sides (59%) had at least one connecting vein between the obturator vein and either the inferior epigastric or the external iliac veins. These communicating veins *always* joined a somewhat larger obturator vein prior to exiting the pelvis through the obturator canal with the obturator nerve. Arterial anastomoses were found less frequently than were venous connections. Thirty-four of 79 approaches (43%) revealed arterial conduits. In all cases only a *single* arterial communication was identified. The arterial system of origin of this vessel was the inferior epigastric in 29 hemipelves (37%) (Figure 1) and the external iliac in the remaining five dissections (6%) (Figure 2). These vessels were not "communicating" vessels as were the veins. In these instances, no proper obturator artery coursed with the obturator nerve and vein. Instead, the retropubic artery *became* the arterial contribution to the obturator neurovascular bundle.

Overall, 58 of 79 sides (73%) had at least one vessel communicating between the obturator system and the external iliac or inferior epigastric systems. Twenty-nine of 79 sides (37%) had more than one vessel. Twenty-one of 79 hemipelves (27%) contained both arterial

and venous conduits. Twenty-five of the 39 pelves available for bilateral examination (64%) had bilateral presence of a communicating vessel. This bilaterality routinely involved different sites of origin of the communicating vessel when the left side was compared to the right. Only seven of 39 pelves (18%) had bilaterally duplicated retropubic vascular anatomy. Thirty-three of 40 left sides (83%) had at least one communicating vessel, whereas only 25 of 39 right sides (64%) had at least one vascular conduit.

Clinical Studies

Retropubic anastomoses were identified in 14 of the 38 cases (37%). Arterial and venous discrimination was unpredictable because the vessels were not traced to their sites of origin. Estimated intraoperative blood loss for the patients with the vessels averaged 1.4 liters, compared to 1.9 liters for those patients in whom an anastomosis was not identified. Evaluation of the fracture anatomy yielded additional important information. Among the 24 cases with no retropubic anastomosis, 14 fractures involved the lateral extent (root) of the superior pubic ramus while four patients had comminuted and displaced quadrilateral surfaces adjacent to the obturator neurovascular groove. Five patients had a communicating vessel as well as a pubic root fracture. Thus, only six of 38 patients (16%) had no retropubic anastomosis and no bony injury in this area. Finally, no obturator nerve injuries were noted at the final follow-up exam.

FIGURE 1 (above): The relationships of arterial and venous communications between the inferior epigastric and obturator systems.

FIGURE 2 (right): The relationships of arterial and venous communications between the external iliac and obturator systems.

Discussion

Retropubic anastomoses between the obturator system and the external iliac or inferior epigastric systems occur more frequently than previously reported. Surgeons should be aware of the high likelihood of encountering at least one communicating vessel along the posterior aspect of the superior ramus when performing the ilioinguinal exposure. The extended Pfannenstiel exposure, popular for pubic symphyseal surgery, also places many of these vessels at risk. These communicating vessels should be separated and controlled to minimize blood loss. Fractures involving the pubic root or quadrilateral surface adjacent to the obturator neurovascular groove are probably less likely to have intact anastomotic vessels and may have more intraoperative bleeding due to these retracted, disrupted vessels, which are difficult to ligate when traumatically torn.

Recommended Reading

Kottmeier S, Farcy J, Baruch H: The ilioinguinal approach to acetabular fracture management. *Oper Tech Orthop*, 3:60-70, 1993.

Letournel E: Acetabulum fractures: Classification and management. *Clin Orthop*, 151:81-106, 1980.

Letournel E, Judet R: *Fractures of the Acetabulum*. New York: Springer-Verlag, 1993.

Matta J, Anderson L, Epstein HPH: Fractures of the acetabulum: A retrospective analysis. *Clin Orthop*, 20:230-240, 1986.

Matta J, Mehne D, Roffi R: Fractures of the acetabulum: Early results of a prospective study. *Clin Orthop*, 205:241-250, 1986.

Mayo K: Surgical approaches to the acetabulum. *Techniques Orthop*, 4(4):24-35, 1990.

Controlled-Release Antibiotic Coatings for Fracture Implants

J. Scott Price, B.Eng.
Allan F. Tencer, Ph.D.
Doug M. Arm, Ph.D.
Greg A. Bohach, Ph.D.

Infection remains one of the most serious complications in the treatment of open fractures, with acute infection or chronic osteomyelitis developing in 5% to 33% of cases. Delivery of antibiotics may be performed systemically or locally with polymethylmethacrylate (PMMA) antibiotic beads. A disadvantage of systemic therapy is the risk of oto- or nephrotoxicity due to high serum antibiotic concentrations. Local antibiotic delivery can reduce this complication by providing a high concentration at the site of need while maintaining low systemic levels. PMMA beads impregnated with antibiotics are used as a local delivery system for established infections and are usually inserted, at the time of debridement of infected bone. PMMA is not degradable so it does not act as a long-term release system, although it does act locally. Further, the beads and wire must be removed after completion of treatment.

We sought to develop a biodegradable coating containing impregnated antibiotics for fracture fixation implants, to be used prophylactically for injuries at risk of infection. Recent research shows that such coatings can act as an effective drug delivery system. Advantages of such an approach would be the provision of a high dose of antibiotic at the site of need early in the course of treatment, a low systemic concentration, maintenance of a therapeutic concentration for up to several weeks, and placement at the time of initial surgery, which could reduce the need for further procedures. We used a stainless steel fracture plate coated with a polylactic-co-glycolic acid copolymer (PLGA) as a biodegradable carrier and Gentamicin as the antibiotic. The study objectives were to establish elution characteristics of antibiotic released from the carrier polymer and to determine if the coated implant would inhibit bacteria growth in vitro.

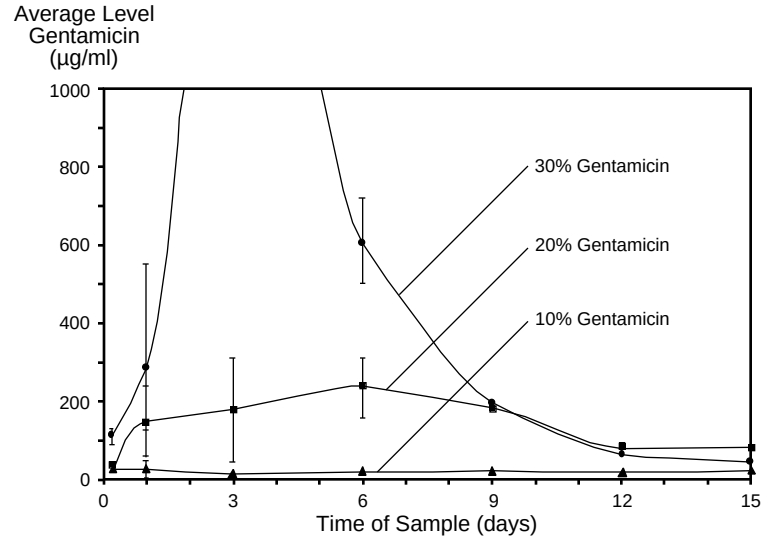

FIGURE 1: Effect of loading concentration on elution characteristics of Gentamicin from coated fracture place.

Methods

Elution Characteristics

PLGA (Medisorb Technologies Inc, Cincinnati, OH) was mixed with Gentamicin (Sigma Inc, St. Louis, MO in a solvent medium. Stainless steel fracture plates (Synthes, Paoli, PA) were coated with the mixture, and the solvent evaporated. The coating was about 0.5 mm thick. An elution study was performed to determine the release kinetics of Gentamicin from the PLGA carrier. Coated implants, prepared using 10%, 20%, and 30% Gentamicin (w/w) were incubated in 10 ml of pH 7.4 phosphate-buffered saline (PBS) at 37°C. The PBS was removed daily, assayed for gentamicin concentration, and replaced with fresh PBS.

Bactericidal Effects

The in vitro model consisted of test tubes containing coated plate sections, about 2 cm long x 1 cm wide immersed in 10 ml of Mueller-Hinton broth. Uncoated plates immersed in similar solution provided the control for comparison. A second control consisted of tubes with no implants at all. Each tube was inoculated with 9.6×10^6 cfu of *Staphylococcus aureus* (ATCC 25923) and incubated at 37°C. Fracture plates were switched to a fresh set of inoculated tubes daily, and the cycle maintained for 24 days. Optical density measurements and colony counts were compared between tubes with coated implants and those with uncoated controls to determine the coating's bactericidal effects.

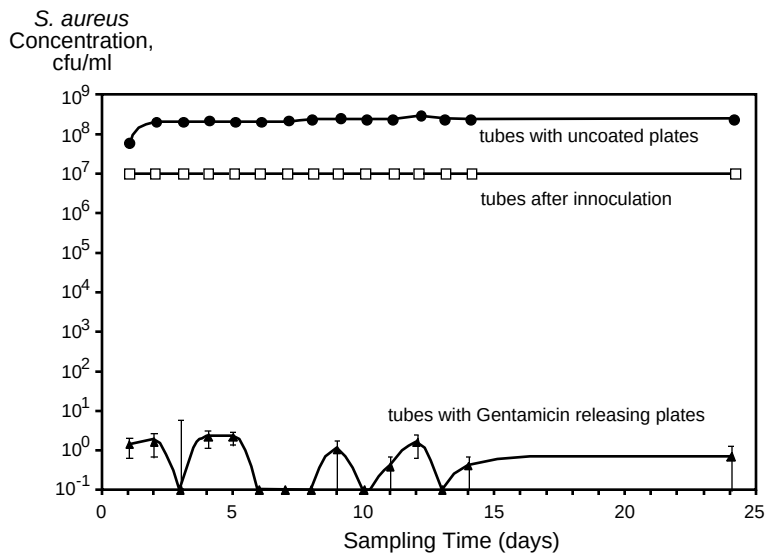

FIGURE 2: Bacterial growth in Gentamicin tubes and control tubes.

Results

Elution Characteristics

Figure 1 illustrates the elution properties of the three concentrations of Gentamicin in the coating. The 20% (Gentamicin / PLGA w / w) films showed an average daily level of 138 mcg / ml over 15 days. This far exceeded the minimum concentration of 1-8 mcg / ml needed to inhibit susceptible organisms. The 10% coating was not selected because its antibiotic levels were too low to be effective in a larger in vivo volume. The 30% coating showed a high-level burst effect between two and four days, but by day 12 output had fallen to the same range as the other coatings, with most of the antibiotic apparently eluted. From in vitro assays, Gentamicin coating concentrations were selected to provide optimum elution over 14 to 21 days of use. Based on the elution profiles, we selected implants coated with 20% Gentamicin and containing a total of 40 mg of Gentamicin per implant.

Bactericidal Effects

The in vitro study showed a significant reduction in bacterial growth in the test tubes containing coated implants compared with the uncoated controls (Figure 2). In control tubes with uncoated implants, a mean concentration of 2.5×10^8 cfu / ml of *S. aureus* was found over 24 days. In control tubes with no implants, the mean concentration was 2.2×10^8 cfu / ml on day 13 when tested. Coated implant tubes averaged only 1.2 cfu / ml. This concentration represented a reduction of more than 99.999% ($p < 0.0001$) from the inoculating dose of 9.6×10^6 cfu.

Conclusion

This study showed that a thin biodegradable implant coating can be developed having bactericidal activity against the organisms frequently associated with osteomyelitis. These implants could be used prophylactically to reduce the incidence of such infections.

Recommended Reading

Arm DM, Tencer AF: Controlled Release of Platelet-Derived Growth Factor from a Biodegradable Film. Fourth World Congress on Biomaterials, Berlin, 1992.

Blaha JD, Calhoun JH, Nelson CL, et al: Comparison of the clinical efficacy and tolerance of gentamicin PMMA beads on surgical wire versus combined and systemic therapy for osteomyelitis. *Clin Orthop Rel Res*, 295:8-12, 1993.

Evans RP, Nelson CL: Gentamicin impregnated polymethylmethacrylate beads compared with systemic antibiotic therapy in the treatment of chronic osteomyelitis. *Clin Orthop Rel Res*, 295:37-42, 1993.

Miclau T, Dahners LE, Lindsey RW: In vitro pharmacokinetics of antibiotic release from locally implantable materials. *J Orthop Res*, 11:627-632, 1993.

Nelson CL, Hickmon SG, Harrison BH: Elution characteristics of gentamicin-PMMA beads after implantation in humans. *Orthopedics*, 17:415-6, 1994.

Norden CW: Antibiotic prophylaxis in orthopedic surgery. *Rev Infec Dis*, Suppl 10, S842-846, 1991.

A Current View of the Scaphoid Nonunion

Peter T. Simonian, M.D.
Thomas E. Trumble, M.D.

Among all wrist injuries, the incidence of fractures of the scaphoid is second only to fractures of the distal radius. Scaphoid fractures comprise 60% to 70% of all carpal bone fractures. It has been estimated that 17,250 to 34,500 nonunions per year will occur despite proper treatment. Nonunions have been attributed to delay in beginning treatment, inadequate immobilization, displacement of the fragments, instability due to ligamentous injury, or inadequate blood supply of the proximal fragment.

Biomechanical studies have demonstrated that the scaphoid plays a key role as the stabilizing link between the proximal and distal carpal rows. Patients with scaphoid nonunions are likely to develop traumatic arthritis with increasing pain, decreased wrist mobility, and weakness. However, the data concerning the natural history of scaphoid nonunions is largely anecdotal and difficult to interpret.

Classification

Scaphoid fractures can be classified according to the time since injury as: acute fracture (less than three weeks old), delayed union (four to six months old), or nonunion (greater than six months old). However, many clinicians diagnose these fractures as nonunions regardless of the time period if sclerosis, cyst formation, or bone resorption is present. Herbert devised a prognostic classification scheme that combines fracture anatomy, stability, and history. Russe classified fractures into three types according to the fracture line relative to the long axis of the scaphoid as: horizontal oblique, transverse, and vertical oblique. Scaphoid fractures have also been classified as distal, waist, and proximal. Fractures of the middle third of the scaphoid are the most common type and have shown a high percentage of delayed unions or nonunions. Proximal pole fractures have a slower rate of healing than do more distal fractures.

Diagnostic Imaging

Early Diagnosis

Because of the incidence of nonunions after occult scaphoid fractures, new methods have recently been investigated to image the scaphoid after injury. Traditionally, scaphoid fracture is assumed if tenderness exists in the anatomic snuff-box, despite negative radiographs. Radiographs are then repeated at 10 to 14 days to determine if a fracture is indeed present. A standard radiographic examination of the suspected scaphoid fracture includes neutral, ulnar deviation, posteroanterior, and lateral radiographs, as well as oblique radiographs made with the wrist in pronation.

In an effort to decrease the delay in diagnosis, which may be warranted in certain patient populations, King and Turnbull recommended that a technetium bone scan be obtained 24 hours after injury. Because this technique is reliable with a reported 100% sensitivity, it can reduce the cost of unnecessary casting and allow early medical clearance for return to work. However, the procedure is relatively time consuming and costly, and it exposes the patient to radiation. The low specificity (75%) of bone scans is improved with clinical correlation.

Displacement and Angulation

Precise imaging of the fracture fragments is difficult because of the complex shape of the scaphoid. Collapse of the fracture fragments is a concern and can be seen on plain radiographs and in more detail with computed tomography. The scaphoid is visualized most completely when six to eight computerized axial-tomographic sections are made along the longitudinal axis of the scaphoid. Computed tomography scans have been used to create three-dimensional models to study scaphoid nonunions, and specifically, the angular relationships of the fracture fragments and volume loss of bone. This loss can vary from 6% to 15% and does not show a linear relationship with the duration of the nonunion. The configuration of the missing bone is consistent, exhibiting a prismatic shape whose base is quadrilateral and faces palmarly. The proximal scaphoid fracture component is extended, radially deviated, and supinated in relation to its distal fracture component.

Avascular Necrosis

Avascular necrosis of the proximal pole of the scaphoid is a negative predictive factor for the success of surgery for the scaphoid nonunion. This is of particular importance in the higher risk elderly and long-standing nonunion populations. It is uncertain if gross examination of the osseous blood supply at surgery correlates with the success of bone grafting. Magnetic resonance imaging studies can detect avascular necrosis in carpal bones and aid in patient selection.

Our Preferred Treatment

We define a scaphoid fracture as nonunion after six months without showing radiographic signs consistent with healing. In the patient less than 40 years old, or if the fracture is less than two years old, we perform bone grafting with internal fixation. We use a dorsal approach when the nonunion is proximal, and a volar approach when the nonunion is at the wrist. We favor use of the Herbert-Whipple (cannulated) screw and derotational K-wire as the form of internal fixation. Magnetic resonance imaging is performed if there is an uncertainty of avascular necrosis. When magnetic resonance imaging is positive for avascular necrosis, we recommend a scapholunate advanced collapse fusion in active patients and a scaphoid excision in the elderly.

In the patient more than 40 years old, or if the fracture is more than two years old, treatment depends on the symptoms. Some patients may be symptomatic. If symptomatic and avascular necrosis is evident, we perform excision arthroplasty, intercarpal fusion, or wrist fusion, depending on the extent and location of osteoarthritis. When there is no radiolunate osteoarthritis, a scapholunate advanced collapse fusion is done. Addition of radioscaphoid and capitate-lunate joint osteoarthritis prompts consideration of a complete wrist fusion.

Recommended Reading

Cooney WP III, Dobyns JH, Linscheid RL: Nonunion of the scaphoid: Analysis of the results from bone grafting. *J Hand Surg*, 5:343-354, 1980.

Gelberman R H, and Menon J: The vascularity of the scaphoid bone. *J Hand Surg*, 5:508-513, 1980.

Kerluke L, McCabe SJ: Nonunion of the scaphoid: A critical analysis of recent natural history studies. *J Hand Surg*, 18A:1-3, 1993.

Osterman AL, Mikulics M: Scaphoid nonunion. *Hand Clin North Am*, 14:437-455, 1988.

Russe O: Fracture of the carpal navicular: Diagnosis, nonoperative treatment and operative treatment. *J Bone Joint Surg*, 42A:759, 1960.

CHIEF RESIDENT PAPERS

Useful Boundaries of the Subacromial Bursa

Timothy C. Beals, M.D.
Mark D. Lazarus, M.D.
Douglas T. Harryman II, M.D.

In 1934, E.A. Codman stated that: "The subacromial bursa itself is the largest in the body and the most complicated in structure and in its component parts. It is in fact a secondary scapulohumeral joint, although no part of its surface is cartilage." Codman attributed great significance to the subacromial bursa in the function of the shoulder. However, it is often regarded with contempt by modern surgeons and acknowledged only as an impediment to visualization of the rotator cuff and a structure worthy of debridement. Recently, interest in this bursa and its role has increased.

This study attempted to identify the anatomic boundaries of the subacromial bursa and determine whether they are useful to the shoulder surgeon. We sought to record the location of the bursa relative to the acromion, acromioclavicular joint, rotator cuff, and most importantly, the axillary nerve. Our primary focus was to define the minimum distance between the most inferior extent of the subdeltoid bursal reflection and the circumflex portion of the axillary nerve and to see whether that relationship can be used as a warning to surgeons splitting the deltoid. We examined anatomic relationships of the subacromial bursa useful for open or arthroscopic approaches to the acromion, subacromial space, rotator cuff, and acromioclavicular joint.

Methods

Eleven fresh-frozen cadaveric shoulders were selected for study. They came from six men and five women whose mean age at death was 68.9 years. Specimens were rejected for evidence of prior surgery or rotator cuff pathology as seen on gross examination during dissection. Taking care not to disturb the bursal tissue, we used a small-gauge needle and gentle traction on the humerus to inject the bursa with a colored latex solution. After injection, we put the glenohumeral joint through gentle range of motion to disperse the latex solution.

The shoulders were kept frozen until the latex had hardened and then were carefully dissected. The examiner used flexible rulers to measure distances between anatomic structures, repeated measurements made, and to confirm recorded values. The glenohumeral joint was in a reduced, neutral-rotation, unelevated position for all measurements.

Results

The mean distance from the anterolateral corner to the posterolateral corner of the acromion was 5.1 ± 0.6 cm. The mean distance from the posterior bursal curtain beneath the acromion to the anterolateral corner was 2.8 ± 0.6 cm. The mean minimum distance from the posterolatera corner of the acromion to the axillary nerve was 5.8 ± 0.9 cm. The mean minimum distance from the midpoint of the acromion to the axillary nerve was 5.7 ± 0.5 cm. The mean minimum distance from the anterolateral corner of the acromion to the axillary nerve was 5.1 ± 0.4 cm. The mean distance from the midpoint of the acromion to the subdeltoid reflection of the subacromial bursa was 4.0 ± 1.0 cm.

The distance between the acromioclavicular joint and the bursa was quite variable, extending from 2.3 cm medial to the joint to three of eleven bursae that did not cross the plane of the joint. The mean distance from the acromioclavicular joint to the bursa margin was 0.7 ± 0.7 cm. The mean distance from the subdeltoid reflection of the subacromial bursa to the axillary nerve was 0.8 ± 0.5 cm with a range of 0 cm to 1.4 cm.

In all specimens, the axillary nerve was no closer to the acromion than the subdeltoid reflection of the subacromial bursa. The mean distance from the midpoint of the acromion to the deltoid insertion was 11.2 ± 1 cm. The examiner observed that the anterolateral corner of the acromion approximated the center of the subacromial bursa with the arm positioned dependently in neutral rotation. The supraspinatus tendon was covered by the bursa in all specimens. The infraspinatus tendon had variable coverage and in several specimens was not covered by the bursa.

Discussion

Fundamental to the practice of surgery is the description of normal anatomy. Although much has been written about the anatomy of the shoulder, relatively little has been written about the region of the subacromial bursa, which occupies the motion interface between the inferior surface of the deltoid and acromion and the rotator cuff and capsule.

To our knowledge, there is no description in the literature of the relationship between the subacromial bursa and the axillary nerve. With the advent of arthroscopic techniques for treatment of acromioclavicular, subacromial, and rotator cuff pathology, this anatomic relationship has a significant effect on the location of arthroscopic portals and the techniques used for surgery.

The goal of this study was to identify practical anatomic relationships that would be helpful to shoulder surgeons performing deltoid splitting approaches and using arthroscopic instrumentation. We showed that in all specimens the axillary nerve was no closer to the acromion than the subdeltoid reflection of the subacromial bursa. This consistent anatomic relationship should be useful to surgeons who incise the deltoid to visualize the acromion and rotator cuff. Our data do not support statements in the literature that the distance from the axillary nerve to the posterolateral corner of the acromion is significantly greater than in other locations or that a defined distance from the acromion can be declared a "safe zone" regarding risk of injury to the axillary nerve.

Another practically useful anatomic relationship identified by our study is that the subacromial bursa occupies the anterior half of the distance between the anterolateral and posterolateral corners of the acromion. This observation has obvious significance to physicians who perform subacromial injections for diagnostic or therapeutic reasons. Furthermore, because the anterolateral corner of the acromion is positioned centrally within the subacromial bursal boundaries, it serves as a useful landmark for accurate placement of a needle or arthroscope into this space.

Recommended Reading

Abbott LC, Saunders JB, Hagey H, et al: Surgical approaches to the shoulder joint. *J Bone Joint Surg*, 31A:235-255, 1949.

Burkhead WZ, Scheinberg RR, Box G: Surgical anatomy of the axillary nerve. *J Shoulder Elbow Surg*, 1:31-36, 1992.

Codman EA: *The Shoulder: Rupture of the Supraspinatous Tendon and Other Lesions in or About the Subacromial Bursa*, 2nd ed. Boston: Thomas Todd, Co., 1934.

Kulkarni RR, Nandedkar AN, Mysorekar VP: Position of the axillary nerve in the deltoid muscle. *Anat Rec*, 232:316-317, 1992.

Strizak AM, Danzig L, Jackson DW, et al: Subacromial bursography. *J Bone Joint Surg*, 64A:196-201, 1982.

Scaphoid Nonunions: AO Cannulated Screws Versus Herbert Screws

Todd Clarke, M.D.
Thomas E. Trumble, M.D.

Since the introduction of the specially designed double-threaded screw by Herbert, we have been using screw fixation and bone grafting to treat displaced acute scaphoid fractures and scaphoid nonunions. Our knowledge of the natural history of scaphoid nonunions is incomplete because the true number of asymptomatic patients is not available in the literature. Amadio and colleagues have published convincing evidence that scaphoid nonunions and displaced acute fractures should be treated provided that scaphoid alignment can be improved. Fractures that healed in a collapsed, malunited position resulted in a twofold increase in the incidence of arthritis.

Internal fixation of scaphoid fractures decreases the time required for immobilization and improves scaphoid alignment. Furthermore, ideal, more accurate placement of internal devices is associated with increased healing rates. We compared patients with scaphoid nonunions treated with a cannulated device versus those treated with a Herbert screw to determine whether a cannulated device allowed us to place our screw more accurately and with any effect on the time to union.

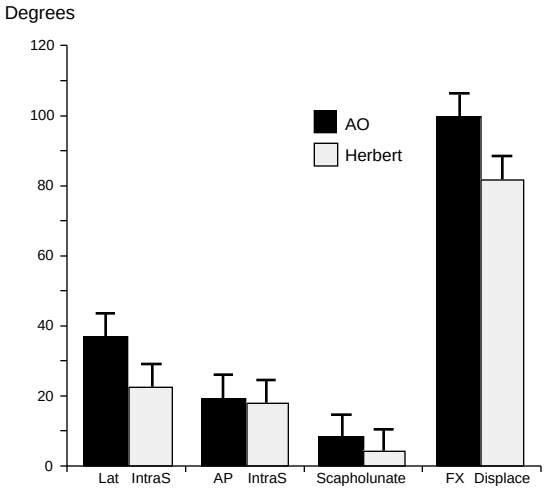

FIGURE 1: With both the AO and Herbert screws there is a significant decrease in the lateral intrascaphoid angle, scapholunate angles, and fracture displacement. The AO Screw provided for statistically significant greater correction of the lateral intrascaphoid angle ($p < 0.005$).

Lat IntraS: lateral intrascaphoid angle
AP IntraS: AP intrascaphoid angle
Scapholunate: scapholunate angle
Fx Displace: fracture displacement measured in millimeters

Method

We treated 48 consecutive patients (mean age, 28 years) with internal fixation and bone grafting of scaphoid nonunions. From 1986-1990 patients were treated exclusively with the Herbert screw. From 1990-1992 they were treated with a 3.5-mm AO cannulated screw. Fourteen patients with either bilateral fractures, fractures involving dislocation of the carpus, or proximal pole fractures requiring a dorsal approach were excluded. We evaluated the remaining 34 patients for time to union, correction of scaphoid alignment, development of arthritis, pain, and placement of the fixation devices using either the AO cannulated screw (n=18) or the Herbert screw (n=16).

We determined the accuracy of screw placement by dividing the proximal pole of the scaphoid into thirds and determining whether the screw was placed in the central third or the peripheral two-thirds. An independent reviewer preoperatively and postoperatively assessed the radiographs. A greater than 50% bridging of the bony trabecula was considered fracture healing. The reviewer measured or noted fracture gap, scaphoid alignment, and avascular necrosis. Functional measurements included range of motion, grip strength, and pain.

Results

The average time to follow-up was 59 months (24-82 months). The delay from fracture to surgical treatment was 13.5 months. The overall union rate was 95% and the time to union averaged 5.3 ± 3.1 months. Time to union with the cannulated AO screws was 3.6 ± 2.5 months versus 7.6 ± 2.6 months, ($p < 0.001$) for patients treated with the Herbert screw. Placement of the cannulated screws was more accurate ($p < 0.01$). There was a significant difference in time to union ($p < 0.0001$) for placement of central screws (5.6 ± 2.1 months) versus peripheral screws (12.8 ± 7.1 months).

Screw fixation with either device provided a significant improvement of the lateral and anteroposterior intrascaphoid angles ($p < 0.01$) (Figure 1). Functional outcome was determined by evaluating range of motion, grip strength, and pain, for which there were no significant differences regardless of the means of internal fixation. The greatest correlation appeared to be the relationship between increasing grip strength (f = 0.69) and improved range of motion (r = 0.74) with decreasing time to union.

In summary, cannulated screw fixation of the scaphoid allows for a more accurate placement and correlates with a shorter time to union. Both fixation devices allow for improved alignment of the scaphoid.

Recommended Reading

Amadio PC, Berquist TH, Smith DK: Scaphoid malunion. *J Hand Surg*, 14A:679-87, 1989.

Cooney WP III, Dobyns JH, Linscheid RL: Nonunion of the scaphoid: Analysis of the results from bone grafting. *J Hand Surg*, 5:343-54, 1980.

Hebert TJ, Fisher WE: Management of the fractured scaphoid using a new bone screw. *J Bone Joint Surg*, 66B:114-23, 1984.

Kleinert JM, Zenni EJ Jr: Nonunion of the scaphoid: Review of literature and current treatment. *Orthop Rev*, 13:19-35, 1984.

Osterman AL, Warhold LG, Maitin EC: Scaphoid nonunion treated with a Herbert screw and bone graft: A prospective study. *J Bone Joint Surg*, (in press).

The Use of Semitendinosus and Gracilis Tendons for Anterior Cruciate Ligament Reconstruction: Three-Year Follow-up Results

Scott E. Hormel, M.D.
Roger V. Larson, M.D
Ivory V. Larry, O.P.A.

Anterior cruciate ligament (ACL) reconstruction is a well-accepted procedure to improve the functional result in patients with ACL-deficient knees. ACL reconstruction using autogenous patellar tendon (PT) has been regarded as the ideal technique. However, attention has been directed to the incidence of complications associated with the use of PT grafts, for example, anterior knee pain, patellofemoral problems, and extensor mechanism weakness.

At the University of Washington Medical Center double loops of semitendinosus and gracilis tendons under arthroscopic control have been used for the past seven years to reconstruct both acute and chronic knees with anterior cruciate insufficiency. This particular technique was selected because it provides a strong intra-articular graft with minimal operative intervention and morbidity.

We report our three-year follow-up results using intra-articular, arthroscopically assisted, autogenous semitendinosus and gracilis tendon (ST/G) reconstruction of the ACL-deficient knee.

Methods

We retrospectively reviewed 50 consecutive patients with unilateral ACL insufficiency who had ACL reconstruction using autogenous ST/G tendon grafts between May 1990 and March 1991. None of the patients had previous ACL reconstruction. Preoperative evaluation included Stryker arthrometric measurement of both knees and radiographs (anteroposterior, lateral, notch, and sunrise views) of the ACL-deficient knee. Diagnostic arthroscopy was performed on each patient, and meniscal tears either debrided or repaired.

The ipsilateral ST/G tendons were harvested and doubled to achieve a graft diameter of 7-9 mm. Following notchplasty, tibial and femoral drill holes were placed in isometric positions as described by Larson and Sidles. The graft was then passed through the tunnels and secured with soft-tissue washers, screws, and sutures (Figures 1 and 2, page 36). Stryker arthrometric measurements were performed on both knees immediately postop, at 12 weeks, 6 months, and at 1 and 3 years using 20 and 30 pounds of force with the knee flexed at 20 degrees to determine the posterior and anterior translation respectively.

Forty-three of 50 patients were contacted three years after surgery; seven patients could not be located. The 31 males and 12 females averaged 29 years of age (range 16-48 years). To eliminate bias, one of our staff members who had no knowledge of patient outcome attempted to contact the subjects. Thirty-seven were available for follow-up and were evaluated using the International Knee Documentation Committee (IKDC), Hospital for Special Surgery (HSS), and Tegner and Lysholm knee evaluation forms. Clinical laxity was objectively analyzed using the Lachman and pivot shift tests, and a Stryker arthrometer. Quadriceps and hamstring strength was evaluated with a Cybex II isokinetic dynamometer at 90 degrees per second. Tunnel placement and determination of compartmental degenerative joint disease were evaluated with radiographs. Six patients were unable to participate in examination and testing, but completed Lysholm and Tegner evaluation forms.

Results

Sixty percent (22/37) of the patients were able to achieve their pre-injury activity level according to the IKDC criteria. With the IKDC subjective and objective assessment, 21/37 (56%) of the patients were graded as normal, 11/37 (30%) nearly normal, 4/37 (11%) abnormal, and 1/37 (3%) severely abnormal (Table 1). Three of the 37 patients had mild harvest site pathology secondary to prominent fixation screws. None of the patients had complaints of patellofemoral pain, quadriceps or hamstring weakness, or instability. There was no difference in outcome between knees reconstructed acutely (less than six weeks) versus chronically.

Based on the HSS criteria (scores range from 0-50), 73% of patients scored 46-50, 24% scored 40-45, 3% scored 35-39, and none scored less than 35. With the Lysholm criteria (scores range from 0-100), 58% scored 90-100, 23% scored 80-89, 9.5% scored 70-79, and 9.5% scored less than 70. On the

Tegner scale, 46% regained their pre-injury level of activity, 28% decreased one level, 7% decreased two levels, and 19% decreased more than three levels.

The average difference between the immediate postop and 12-week laxity of the reconstructed graft based on Stryker arthrometry measurements was 1.4 mm (range, -0.66 to +4.66 mm). The average difference between the 12-week and one-year laxity was 0.7 mm (range, -1.33 to +3 mm), whereas the average difference between the one-year and three-year laxity measurement was 0.4 mm (range, -3 to +4.66 mm). The average laxity difference between the reconstructed and contralateral knee at one- and three-year follow-up was 1 mm (range 0 to 2.66 mm) and 1.1 mm (range 0 to 4.0 mm), respectively. Eighty-eight percent of the patients had a side-to-side difference between 0 and 3 mm. Isokinetic quadriceps and hamstring peak torque of the reconstructed knee compared to the contralateral knee was 91% (range 69-102%) and 90% (range 40-111%), respectively. The average hamstring quadriceps ratio of the reconstructed side and contralateral side was 71% (range 37-97%) and 71% (range 55-88%), respectively.

Radiographs obtained at the three-year follow-up demonstrated no consistent degenerative changes or positional changes in the femoral or tibial drill holes or hardware. Meniscal pathology was commonly observed in our patient population at the time of diagnostic arthroscopy. Twenty-six of 37 patients had meniscal tears. Three meniscal tears were repaired and the rest debrided. Two of the five abnormal or severely abnormal results occurred in patients without any meniscal pathology. However, one of these patients had a large area of full-thickness cartilage loss from the medial femoral condyle, and the other had an associated medial collateral ligament tear (grade III).

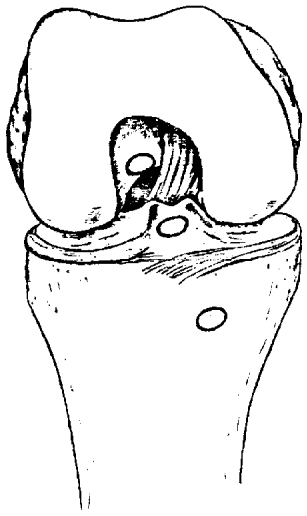

FIGURE 1: Diagram showing isometric position of tibial and femoral tunnels.

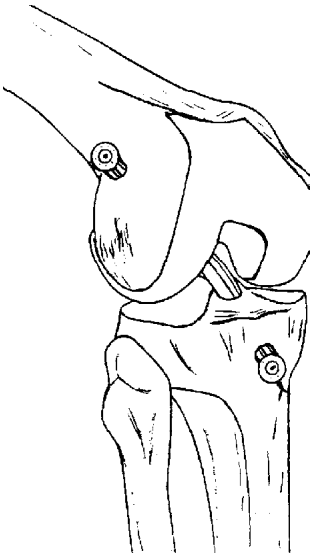

FIGURE 2: Diagram showing an ACL graft secured with soft-tissue washers and screws.

Discussion

Numerous authors have reported the use of semitendinosus and gracilis tendon autografts for reconstruction of the anterior cruciate ligament. Our rationale for the use of doubled-looped ST/G graft was based on the in vitro tensile strengths of various tissues used for ACL reconstruction as reported by Noyes in 1984, as well as the side effects reported in patients who had ACL reconstruction using patellar tendon grafts. In fact, the use of hamstring grafts may offer several advantages over other commonly used autografts such as the patellar tendon. The potential advantages of these looped hamstring grafts include increased strength, stiffness characteristics similar to the normal ACL, a large surface area for revascularization, ease of tensioning, adaptability to precise positioning, and decreased surgical morbidity.

We sought to perform a comprehensive study using established subjective and objective criteria to evaluate the three-year follow-up results of ACL reconstructions using ST/G tendon graft. Evaluation of our patients with four different grading systems, arthrometry, and dynometry enabled us to compare our results with those of other published ACL studies that used patellar tendon and other autogenous grafts.

In our series, we had no complaints of hamstring harvest-site morbidity, hamstring weakness, or anterior knee pain. These results support the findings of Yasuda, who also reported minimal morbidity with ST/G grafts. These data contrast with a recent study by Marder in which up to 24% of the patients (both ST/G and PT graft reconstructions) experienced anterior knee pain. Three patients in our study complained of mild discomfort as a result of prominent hardware.

Overall, we had excellent or good results in approximately 80-86% of the patients as determined by the four grading criteria. Sixty percent were able to achieve their pre-injury activity level, or a level with which they were satisfied. However, this percentage varied between the IKDC and Tegner criteria, perhaps partly due to the complexity of the Tegner criteria form, which patients had difficulty understanding.

A recent study by Rosenberg demonstrated that only 30% of the patients reconstructed with PT grafts were able to return to their pre-injury level despite having a stable knee with normal strength. There was no observable difference in grade or outcome between patients who had reconstructions done acutely or chronically. Of the five patients with poor results, two had traumatically injured the reconstructed knee and had objective findings that lowered their overall grades. The other three received a poor grade as a result of subjective complaints consisting of diffuse pain, catching, and decreased activity.

We also demonstrated that if overtensioned, a majority of the hamstring grafts adapted within the first 12 weeks following surgery with minimal increased laxity thereafter. The average increase in tendon length was 1.4 mm within the first 12 weeks compared to an increase of only 0.4 mm between one and three years. These data support other studies that refute the speculation that hamstring grafts may continue to stretch and become lax over time. Furthermore, the average anterior laxity difference between the reconstructed and contralateral knee at one and three years remained constant at approximately 1.1 mm, and 88% had a side-to-side difference of between 0 and 3 mm. This is a much smaller difference compared to some reports of patellar tendon grafts in which only 46% (Frogameni), 57% (Aglietti), and 69% (Shino) had a side-to-side difference of 0-3 mm and an average of 1.7 mm of laxity (Rosenberg). Finally, our results measuring quadriceps and hamstring strength were comparable to other studies using hamstring grafts. Although there have been studies demonstrating significant hamstring weakness following ST/G harvesting, our patients failed to demonstrate such weakness. Studies using patellar tendon grafts have shown the quadriceps peak torque at 60 degrees per second to range from 66% to 85% of the contra lateral side compared to our results of 91%.

Although our patients had a wide range of quadriceps and hamstring peak torque values, they reported no subjective complaints of weakness and showed no evidence of weakness on clinical examination. Furthermore, Cybex testing at our institution is performed at 90 degrees per second to reduce the general stress on the patella-femoral joint. Testing at 60 degrees per second usually results in higher peak torques, so we can compare our patients and those studied at 60 degrees per second.

TABLE 1: International Knee Documentation Committee (IKDC) Grading

	Normal	Normal	Near Abnormal	Severe Abnormal
Medial meniscal debridement	6	2	0	0
Lateral meniscal debridement	3	1	2	0
Med & lat menis debridement	5	3	1	0
Meniscal Rrpair	2	1	0	0
No Meniscal pathology	5	4	1	0
Other	0	0	0	1*
Total	21/37	11/37	4/37	1/37

* Medial femoral condyle cartilage defect

Conclusions

1. Knee instability as a result of ACL insufficiency or rupture can be successfully reconstructed acutely or chronically using double-looped ST/G grafts.
2. Subjective and objective results in our patients reconstructed using ST/G grafts compared favorably to other studies using patellar tendon and hamstring grafts.
3. Harvest site morbidity, complaints of hamstring weakness, or patellofemoral pain are extremely rare in patients reconstructed with ST/G grafts.
4. If overtensioned, hamstring grafts will adapt during the first 12 weeks. There was no evidence suggesting length change past one year. Therefore, grafts that are clinically stable at one year postoperatively are likely to remain stable.
5. Ipsilateral hamstring and quadriceps strength was approximately 90% of the contralateral side. There was no evidence to suggest significant hamstring weakness at three-year follow-up due to the loss of the ST/G tendons.
6. Most of the patients with poor results tended to have subjective complaints with few objective abnormalities. Therefore, overall outcome did not appear to be related to technical error. Poor results may be related to other internal derangements (e.g., meniscal tears, early degenerative joint disease), or psychological profiles. We believe that most patients with excellent outcomes were either competitive athletes or highly motivated persons who maximally participated in their postoperative rehabilitation program. *(continued on page 39)*

Investigation of High-Energy Phosphate Levels in Normal and Diabetic Skin

William J. Mills, M.D.
Douglas G. Smith, M.D.
Sigvard T. Hansen Jr., M.D.
Grant Steen, Ph.D.
David Williams, Ph.D.

Predicting and measuring tissue viability remains a challenge to the orthopedic surgeon. The management of diabetic and dysvascular patients with lower limb ischemia is particularly challenging. Clinical assessment and judgment of optimal levels of wound healing are imperfect; similarly, great effort can be expended treating superficial wounds and deep infections when treatment is ultimately destined to fail due to poor perfusion of the involved extremity.

In the past decade, several noninvasive methods have been designed to assess preoperatively the potential for wound or amputation healing. Ankle perfusion pressures are inconsistent in predicting wound healing in the diabetic patient. Some surgeons, but not others, have found transcutaneous oxygen tension a useful predictor of successful wound healing after amputation. Indirect measures of nutritional status, including serum albumin levels and total lymphocyte counts, are helpful adjuncts to predict wound healing following amputation.

Until recently, all attempts at predicting wound healing or assessing tissue viability have centered on indirect measures, either of tissue perfusion, oxygen delivery, or general nutritional status. Now, nuclear magnetic resonance (NMR) spectroscopy technology is available to measure phosphate substrates in specific organs and tissues, including brain, heart, kidney, liver, and skeletal muscle.

It is well established that cellular injury and ischemia lead to altered and quantifiable patterns in phosphorous spectra in compromised tissues. It has been possible to quantify the levels of adenosine triphosphate (ATP), adenosine diphosphate (ADP), phosphocreatine (PCr), and inorganic phosphate (Pi) in living tissue. Measurement of these essential substrates and byproducts of cellular energy metabolism allows a more direct assessment of the energy potential of individual tissues for such activities as wound healing.

Methods

In the past, measurement of phosphorous spectra from the skin was hampered by unwanted signal from underlying soft tissues and skeletal muscle. Recently, however, a surface coil was developed capable of measuring phosphorous spectra from skin only and rejecting the signal from underlying tissues. We used this coil to compare the phosphorous spectra from the dorsal foot skin of a control group of six normal volunteers with spectra obtained from a group of six patients with diabetes and limbs at risk. We selected this site because the foot is the most frequent location for complications of chronic ulceration and poor wound healing in this patient population.

The data generated with NMR spectroscopy is a measure of the relative abundance of ATP, ADP, PCr, and Pi in the skin. The ^{31}P molecules in skin resonate within the magnet at a characteristic frequency. Each time the tissue is probed by the skin coil a characteristic radio frequency signal is emitted by the excited ^{31}P atoms in high-energy compounds. Because the computer hardware produces a back-ground noise that can obscure the ^{31}P spectra with individual probes, the tissue is probed multiple times to distinguish the distinct spectral pattern of ATP, ADP, PCr, and Pi from the static background signal or "noise." As the background noise is a constant, the signal-to-noise ratio is a useful means of comparing the relative abundance of different compounds.

Results

In control skin, spectral resonances are present for ATP and PCr, but the Pi resonance is statistically indistinguishable from background noise. In diabetic spectra, resonances are present for Pi as well as ATP and PCr. Spectra from diabetic skin resembles that from normal skin that has been rendered temporarily ischemic by application of a tourniquet. The relative abundance of Pi in diabetic skin spectra suggests that the skin suffers chronically from inadequate perfusion.

With our current protocol, the ATP signal-to-background noise ratio for the largest spectral resonance is

TABLE 1: Resonances of phosphorous spectra measured in the skin

	ATP	PCr/ATP	
	Signal/Noise	Pretreatment	After Nicotine
Controls	15.92	3.13	2.57
Diabetics	2.25	.95	.24
	$p <$. 001	$p <$. 01	$p <$ .001

>10 in all control subjects, but <3 in all diabetic subjects (Table 1). This signal-to-noise difference permits us to discriminate between normal and diabetic skin. The signal-to-noise ratio is proportional to the concentration of metabolites present, and strongly suggests that the overall concentrations of bioenergetic metabolites in diabetic skin are reduced by as much as 90% compared to normal skin.

Skin bioenergetic status was further quantified as the ratio of PCr to ATP, because this ratio allows us to directly compare diabetic to normal skin. The energy metabolism of tissue is intimately related to the turnover rate of intracellular compounds containing high-energy phosphate bonds. The hydrolysis of ATP is prominent in the pathway converting potential energy to cellular activity, while Pcr is an important shuttle for ATP within the cell.

In normal oxidative conditions, as energy is consumed, ATP and PCr should decline in parallel. It has been reported that in hypoxic tissues the decrease in PCr as it is converted to lactate is not accompanied by a clear decrease in ATP. The relative PCr / ATP ratio is therefore an indication of the relative aerobic or ischemic state of tissues. Our findings suggest that this ratio differed significantly in the unchallenged situation, as well as following the chewing of nicotine gum. Following nicotine gum, the ratio of PCr to ATP declined an average of 23% in controls, but more than 74% in the diabetics.

Recommended Reading

Cady EB: *Clinical Magnetic Resonance Spectroscopy*. New York: Plenum Press, 1990.

Dickaut SC, Delee JC, Page CP: Nutritional status: Importance in predicting wound healing after amputation. *J Bone Joint Surg*, 66A: 71-75, 1984.

Golbranson FL: The use of skin temperature determination in lower extremity amputation level selection. *Foot Ankle*, 3:170-177, 1982.

Klein HW, Gourley IM: Use of magnetic resonance spectroscopy in the evaluation of skin flap circulation. *Ann Plast Surg*, 20:547-551, 1988.

Wyss CR, Harrington RM, Burgess EM, Matsen FA: Transcutaneous oxygen tension as a predictor of success after an amputation. *J Bone Joint Surg*, 70A: 203-207, 1988.

ACL Reconstruction

(from page 37)

Recommended Reading

Agilietti P, Buzzi R, et al: Patellar tendon versus doubled semitendinosus and gracilis tendons for anterior cruciate ligament reconstruction. *Am J Sports Med*, 22(2):211-218, 1994.

Hughston JC: Complications of anterior cruciate ligament surgery. *Orthop Clin N Am*, 16:237-240, 1985.

Larson RV: Arthroscopic ACL reconstruction utilizing double-loop semitendinosis and gracilis tendons. In: *Book of Abstracts, Instructional Courses and Symposia*, 11th Annual Meeting, Arthroscopy Association of North America, Boston, 1992, pp. 124-128.

Marder RA, Rasking JR, Carrol M: Prospective evaluation of arthroscopically assisted anterior cruciate ligament reconstruction: Patellar tendon versus semitendinosus and gracilis tendon. *Am J Sports Med*, 19(5):478-484, 1991.

Otero AL, Hutcheson L: A comparison of the doubled semitendinosus, gracilis and central thrid of the patellar tendon autografts in arthroscopic anterior cruciate ligament reconstruction. *Arthroscopy*, 9(2):143-148, 1993.

Steiner ME, Hecker AT, et al: Anterior cruciate ligament graft fixation. Comparison of hamstring and patellar tendon grafts. *Am J Sports Med*, 22(2):240-247, 1994.

Yasuda K, Ohkoshi Y, et al: Morbidity cuased by autogenous semitendinosus and gracilis tendon graft harvest. Presented at the 1994 Annual Meeting of the American Academy of Orthopaedic Surgeons, New Orleans.

The Role of Bone Scans for Evaluating Bony Lesions

Ron Kristensen, M.D.
Ernest U. Conrad III, M.D.

Technetium bone scans are widely used in evaluating abnormal radiographs, pain of uncertain etiology, and in evaluating for a secondary lesion with a known primary tumor. While studies to date have not found scintigraphy to be pathognomonic in differentiating benign from malignant lesions, many clinicians believe the pattern of the uptake is suggestive for various tumors. McLean, Pearlman, Murray, and Goodgold all found a correlation between the bone scan and certain bony tumors. Other authors, such as Berg, found such variability within each tumor type that no definitive diagnosis could me made based upon the scintigraphic findings. In an attempt to improve the specificity of this modality, Sneppen in 1978 used quantitative bone scanning. To obtain a quantitative scan, an area of interest is defined and compared to an area of equal size to obtain a ratio. Sneppen found that lesions with low uptake were more likely to be benign, but found enough variability that he concluded bone scanning was unable to differentiate benign from malignant lesions.

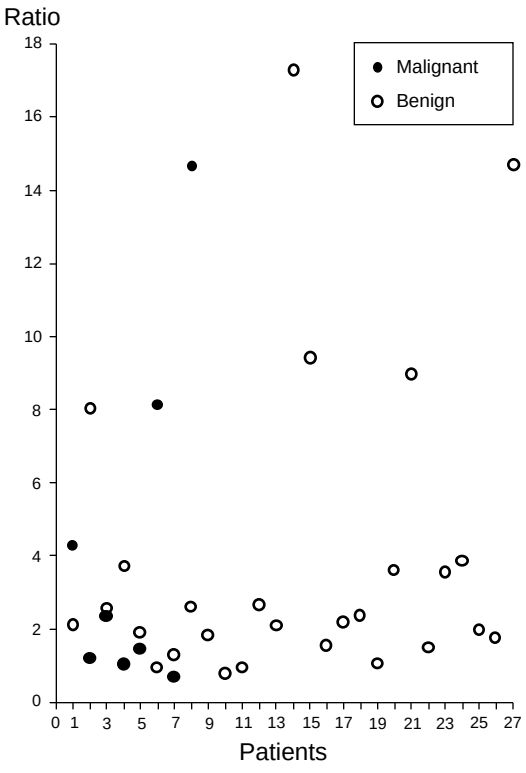

FIGURE 1: Scatter diagram of the ratios of the malignant lesions (filled circles) and benign lesions (open circles).

Our study attempted to improve upon the work of Sneppen by using modern scanners and combining the scinitgraphic information with the radiographic information. As an abnormal bone scan frequently prompts a cascade of tests including CT, MRI, and even a biopsy, and our goal was to limit the number of patients that required such exhaustive evaluation.

Methods

This project studied all children with a radiographic abnormality who were referred since August 1992 to the orthopedic oncologist at Children's Hospital and Medical Center in Seattle. We used the same scanner to perform scintinography on all children and defined an area of interest as the area of maximal uptake. This area of uptake was converted to a ratio by comparing it to an area of identical size on the contralateral limb. In addition, we classified the radiographic abnormalities based upon their bony destruction, periosteal reaction, and matrix formation. In most cases, the diagnosis was confirmed by the pathologic specimen.

Results

The orthopedic oncology service at Children's Hospital evaluated more than 300 patients during the study period. Thirty-four of these patients, 21 boys and 13 girls, met all the criteria: a radiographic abnormality, a bone scan at Children's Hospital, and a pathologic specimen to confirm the diagnosis. The average bone scan ratio for the 26 benign lesions was 3.49 ± 3 .67 with a range of 9.96 to 17.38; if the axial skeleton is excluded the average is 3.61 ± 4.04 (0.96 to 17.38). For the eight malignant lesions, the average was 4.25 ± 4.91 (0.69 to 14.75), and without the axial skeleton, the average was 6.97 6.01 (0.69 to 14.75). Figure 1 plots the bone scan ratios. When this information was calculated for the area of hottest uptake, the benign lesions had a mean 3.13 ± 3.1, and without pelvis 3.45 ± 3.37. Malignant lesions had a ratio of 2.78 ± 2.67 and 5.11 ± 3.4 without the axial skeleton.

All of the malignant lesions in the extremities were metaphyseal or met-diaphyseal. Further, only one of the malignant lesions was of mixed density. The osteosarcomas showed increased density and the Ewings sarcomas decreased density. All the malignant lesions were poorly marginated except for the chondrosarcoma, which was intermediate.

Conclusion

The strict inclusion criteria for this study did not provide the number of patients needed to draw statistically significant conclusions. We found that the wide variability in bone scan ratios in both benign and malignant lesions did not allow us to differentiate benign from malignant lesions. The radiograph was the most helpful tool for differentiating benign from malignant lesions.

Recommended Reading

Simon MA: Scintigraphic evaluation of primary bone tumors. *J Bone Joint Surg*, 62A:758-764, 1980.

Sneppen O: Numerical assessment of bone scintigraphy in primary bone tumors and tumor-like conditions. *J Bone Joint Surg*, 60A:966-969, 1978.

— National Research Grants —

Department of Orthopaedics

F National Institutes of Health (NIH)

Collagens of Cartilage and the Intervertebral Disk — *David Eyre*

Imaging of Molecules by Oscillator-Coupled Resonance — *John Sidles*

Regulation of Gene Expression in Cartilage — *Linda Sandell*

Pathology of Inborn Skeletal Diseases — *David Eyre*

Premorbid Risk Factors for Back Disorders vs. Absenteeism — *Stanley Bigos*

Spine Pathology and LBP Determinants in Identical Twins — *Michele Battié*

Development of an Extremity Trauma Outcome Scale — *Marc Swiontkowski*

F Veterans Affairs Medical Center Review Grants

Biomechanics of Hindfoot Fusion — *Bruce Sangeorzan and Allan Tencer*

Synthesis and Function of Cartilage Matrix Molecules — *Linda Sandell*

F Centers for Disease Control and Prevention Injury Prevention Grant

Spinal Canal Geometry Changes in Vertebral Fracture — *Allan Tencer*

F Orthopaedic Research and Education Foundation (OREF)

Hereditary Multiple Exostoses:
Mapping the Genes for a Skeletal Dysplasia — *Ernest Conrad*

Randomized Multicentered Clinical Trial of Distal Radius
Fracture Treatment — *Hans Kreder*

Biomechanics of Femoral Neck Fixation — *Jens Chapman*

Contributors to Departmental Research and Education

May 1994 Through April 1995

We express our appreciation to all who have contributed to the work of the Department of Orthopaedics over the past year. Your assistance makes possible special research activities, educational programs, and other projects that we could not carry out without this extra support from our alumni, faculty, and friends in the community. We owe a special thanks to the University of Washington Resident Alumni who have made significant contributions to help further the education of our current residents.

Alumni & Residents

Class of '52
Park W. Gloyd

Class of '63
Alfred I. Blue

Class of '64
Harold J. Forney
Theodore K. Greenlee
David E. Karges

Class of '68
Lynn T. Staheli

Class of '69
Edward E. Almquist
Sigvard T. Hansen, Jr.
Edward L. Lester
Hugh E. Toomey

Class of '70
John C. Brown
Malcom B. Madenwald

Class of '71
Bruce E. Bradley, Jr.

Class of '72
Thomas L. Gritzka
David R. Nank
John A. Neufeld

Class of '73
Theodore A. Wagner

Class of '74
Richard A. Dimond
Ronald B.H. Sandler

Class of '75
Thomas M. Green
Frederick A. Matsen III
Donald Plowman
Robert A. Winquist

Class of '76
Douglas T. Davidson
Richard A. Zorn

Class of '77
Larry D. Iversen
Mark C. Olson

Class of '78
Gary J. Clancy
Arnold G. Peterson

Class of '79
Allan W. Bach
Jonathan L. Knight
Richard L. Semon

Class of '80
John M. Hendrickson
Michael A. Sousa

Class of '81
John M. Clark
Dennis J. Kvidera
Martin S. Tullus
Robert G. Veith

Class of '82
Richard M. Kirby
Steven S. Ratcliffe

Class of '83
Robert M. Berry
Edward L. Farrar, III
Keith A. Mayo
Elizabeth A. Ouellette
Henry K. Yee
Joseph D. Zuckerman

Class of '84
Jeffrey W. Akeson
Thomas J. Fischer
Marc F. Swiontkowski

Class of '85
Paul J. Abbott
William P. Barrett
Richard J. Barry
Daniel Flugstad
Jeffrey N. Hansen

Class of '86
Gary D. Bergman
Lawrence Holland
Carlton A. Keck, Jr.
Michael E. Morris

Class of '87
Craig T. Arntz
Herb R. Clark
Michael K. Gannon

Class of '88
Jonathan L. Franklin
Michael A. Thorpe
Richard V. Williamson

Class of '89
James P. Crutcher, III
Martin G. Mankey
Steve C. Thomas

Class of '90
Ken Fujii
David M. Kieras
Walter F. Krengel, Jr.
Jay A. Winzenried

Class of '91
David H. Bishop
Timothy Lovell
Kit M. Song
Mark C. Remington

Class of '92
Elisha T. Powell
Michael J. Sailer
Jeffrey L. Stickney
Donald B. Striplin

Class of '93
Philip J. Kregor
Susan R. Schmitt
Lyle S. Sorensen
J. Eric Vanderhooft

Class of '94
Eric J. Bowton
Sohail K. Mizra
William T. Obremskey
James W. Vahey
P. Brodie Wood

Class of '95
Timothy C. Beals
B. Todd Clarke
Scott E. Hormel
Ronald M. Kristensen
William J. Mills

Class of '96
Vernon J. Cooley
David A. Deneka
Peter W. Mitchell
Peter T. Simonian
William F. Wagner

Class of '97
Laddie A. Agtarap
Mohammad Diab
David G. Levinsohn
Daniel J. Stechschulte
Randall W. Viola

Class of '98
David J. Belfie
Jay L. Crary
Oriente DiTano
Donald P. Ericksen
Colin E. Poole

Faculty and Friends of Orthopaedics

George Aagaard
Elizabeth Abu-Haydar
Samuel G. Agnew
American College of Foot & Ankle Surgery
David W. Anderson
Paul A. Anderson
Ankle & Foot Clinic
Barbara L. Baugh
Stephen K. Bernirschke
Paul J. Benca
Stanley J. Bigos
Biomet, Inc.
Bruce G. Blackstone
William A. Boegel
Lawrence B. Bone
James Bouchard
Richard Bouche
Thomas R. Boyce
Bruce E. Bradley, Jr.
Paul Wilson Brand
David and Christine Brokaw
John & Louise Bryson
John F. Buckmiller
Ernest M. Burgess
R.B. & Colleen Calkins
James Carr
Len C. Ceder
Richard Chandler
Jens R. Chapman
Jeffery Christensen
D.K. Clawson
Michael Coe
Dr. and Mrs. Ernest U. Conrad
Richard Conrad
Michael K. Copass
Charles Cornell
Howard B. Cotler
Kathryn E. Cramer
Steve Czick
Mark C. Dales
Charles B. Davis
Thomas Decoster
Jonathan Deland
Depuy, Inc.
Gary L. Dockery
EBI Medical Systems
Michael Egglin
Benjamin L. Ellison
David R. Eyre
David E. Fairbank
Edward Farrar
Professor Ganz
R. Garo
Thomas Gedgaudas
James J. Ghiglione
J.T. Giesen
Paul Grainger
George & Marilyn Gruber
Douglas P. Hanel
Christopher M. Hansen
Eric T. Hansen
Marilee Hansen
Douglas T. Harryman
Joseph M. Hendrickson
M. Bradford Henley
Howmedica
Innovative Surgical Devices
Sarah Jackins
Robert Jackson
Wells C. Jacobson
Diana J. Jansen
Vivian Jenkins
Andrew Jonassen
Jesse Jupiter
David M. Kaehr
Thomas L. Kalivas
Jonathan P. Keeve
Keolker & Swerk
Tom Kimmel
Howard A. King
Reginald Q. Knight
Stephen Kittmeier
Justin LaMont
Richard Lange
Roger V. Larson
Harold Laws
Steven LeBaron
Rebecca Lessard
James P. Logerfo
David C. Loken
Ruedi Maag
Ronald V. Maier
Leon H. Malkin
Peter R. Mandt
Arthur Manoli
David A. Maquire
Randall Marcuss
Rene K. Marti
Brenda McFetridge
Robert C. McGill
William C. Meade
Mark Meier
Berton R. Moed
Vincent S. Mosca
Carol A. Mowery
Daniel L. Moye
M.E. Müller
John A. Neufeld
Stanley G. Newell
Joanne H. Nielson
Edward R. North
Wolfgang Oettinger
Susan Olson
Robin and Bettina Peter
Arnold Peterson
Elisha Powell
Howard N. Putter
Leslie Quinn
Romano Surgical Instruments
Harry S. Reese
Hansjorg Reimer
Paul H. Reiss
John V. Rice
Louis Rioser
James R. Robbins
Lawrence R. Robinson
Ray & Elizabeth Robinson
Milton L. (Chip) Routt
John T. Sack
Kent Saltonstall
Linda J. Sandell
Richard Sandler
Andrew Sands
Bruce J. Sangeorzan
Vincent Santoro
Seattle Plastic Surgeons
Hugh S. Selznick
Stephen R. Shimer
Douglas G. Smith
Judith W. Smith
John E. Stewart
Edward Stokel
Donald Striplin
Jos Styuck
Synthes (Wyss)
Allan F. Tencer
Charles Thomas
Steven C. Thomas
Martin Tile
H.E. Toomey
Thomas E. Trumble
H. Tscherne
William Turner
James Vahey
J. L. Vander Schilden
Nicholas B. Vedder
Peter J. Verdin
Washington State Podiatric Medical Association
Larry Webb
Michael J. Weber
Lowell Scott Weil
Gregory West
Richard & Deborah Winn
John Wilber
Hans Willenegger
Robert P. Wills
David Miller Wise
Robert Woutat
Hansjorg Wyss

Department of Orthopaedics

Faculty

Frederick A. Matsen III, M.D.
Professor and Chair

Michele C. Battié, Ph.D.
Research Associate Professor
Stephen K. Benirschke, M.D.
Associate Professor
Stanley J. Bigos, M.D.
Professor
James T. Bruckner, M.D.
Assistant Professor
Howard A. Chansky, M.D.
Acting Instructor
Jens R. Chapman, M.D.
Assistant Professor
John M. Clark Jr., M.D., Ph.D.
Associate Professor
Ernest U. Conrad III, M.D.
Associate Professor
David R. Eyre, Ph.D.
Professor
Theodore K. Greenlee Jr., M.D.
Associate Professor
Douglas P. Hanel, M.D.
Associate Professor
Sigvard T. Hansen, Jr., M.D.
Professor
Douglas T. Harryman II, M.D.
Associate Professor
M. Bradford Henley, M.D.
Associate Professor
Roger V. Larson, M.D.
Associate Professor
Vincent S. Mosca, M.D.
Associate Professor
Milton L. Routt Jr., M.D.
Associate Professor
Linda J. Sandell, Ph.D.
Professor
Bruce J. Sangeorzan, M.D.
Associate Professor
John A. Sidles, Ph.D.
Associate Professor
Douglas G. Smith, M.D.
Assistant Professor
Lynn T. Staheli, M.D.
Professor
Marc F. Swiontkowski, M.D.
Professor
Carol C. Teitz, M.D.
Associate Professor
Allan F. Tencer, Ph.D.
Associate Professor
Thomas E. Trumble, M.D.
Associate Professor
Jiann-Jiu Wu, Ph.D.
Research Associate Professor

Adjunct Faculty

Basia R. Belza, R.N., Ph.D.
Assistant Professor
Physiological Nursing
Anne-Marie Bollen, Ph.D.
Assistant Professor, Orthodontics
Charles H. Chesnut III, M.D.
Professor, Nuclear Medicine
Gregory C. Gardner, M.D.
Assistant Professor, Rheumatology
Thurman Gillespy, M.D.
Associate Professor, Radiology
Daniel O. Graney, Ph.D.
Associate Professor
Biological Structure
Laurence A. Mack, M.D.
Professor, Radiology
Susan M. Ott-Ralph, M.D.
Associate Professor
Division of Metabolism
Wendy Raskind, M.D., Ph.D.
Associate Professor
General Internal Medicne
Michael L. Richardson, M.D.
Associate Professor, Radiology
Peter A. Simkin, M.D.
Professor, Medicine

Joint Faculty

John E. Olerud, M.D.
Professor, Division of Dermatology
Stephen G. Rice, M.D., Ph.D.
Lecturer, Pediatrics
Nicholas B. Vedder, M.D.
Assiociate Professor
Plastic Surgery

Affiliate Faculty

David A. Boone, C.P., *Director and Co-Principal Investigator, Prosthetics Research Study*
Sarah E. Jackins, R.P.T.
Rehabilitation Medicine

UNIVERSITY OF WASHINGTON SCHOOL OF MEDICINE

Department of Orthopaedics
University of Washington
Box 356500
Seattle, Washington 98195-6500

Phone: (206) 543-3690
Fax: (206) 685-3139

Affiliated Institutions

Children's Hospital and Medical Center
4800 Sand Point Way NE
Seattle, WA 98105
(206) 526-2109

Harborview Medical Center
325 Ninth Avenue
Seattle, WA 98104
(206) 223-3466

University of Washington Medical Center
Bone and Joint Center
4245 Roosevelt Way NE
Seattle, WA 98195
(206) 548-4288

Veterans Affairs Medical Center
1660 South Columbian Way
Seattle, WA 98108
(206) 764-2215